Sequential Analysis: Optimization of Substructure Technique - Minimization of Differential Column Shortening and Result Approximation by ANN

Njomo Wandji Wilfried

Submitted to the
Institute of Graduate Studies and Research
in partial fulfillment of the requirements for the Degree of

Master of Science
in
Civil Engineering

Eastern Mediterranean University
January 2013
Gazimağusa, North Cyprus

Approval of the Institute of Graduate Studies and Research

Prof. Dr. Elvan Yılmaz
Director

I certify that this thesis satisfies the requirements as a thesis for the degree of Master of Science in Civil Engineering.

Asst. Prof. Dr. Mürüde Çelikağ
Chair, Department of Civil Engineering

We certify that we have read this thesis and that in our opinion it is fully adequate in scope and quality as a thesis for the degree of Master of Science in Civil Engineering.

Asst. Prof. Dr. Giray Özay
Supervisor

Examining Committee

1. Asst. Prof. Dr. Giray Özay
2. Asst. Prof. Dr. Erdinç Soyer
3. Asst. Prof. Dr. Serhan Şensoy

ABSTRACT

This thesis deals with sequential analysis coupled with an optimized substructure technique modeled on 3D-frame construction process. This model handles the hypothesis that any subpart of the entire structure can be constructed at a time. On a realistic 3D-frame building, permanent gravity load (dead load), variable gravity loads (construction load, live load) and non-gravity loads or effects (time dependence, temperature, and earthquake) are either applied sequentially or following the conventional method. Their individual contributions on bending moments, key of design, are investigated. To implement this analysis, some additional computational efforts can be justified. Though, an optimized procedure using substructure technique is proposed, based on a smart but simple choice of the substructure size. The proposed procedure intends to minimize the required memory used while reducing the required time as well. The sequential analysis as presented herewith reveals many salient features and more accurate results that should be employed in analyzing buildings, more so tall ones.

However, in the preliminary design stage of a RC 3D-frame, repeated sequential analyses to determine optimal members' sizes and the investigation of the parameters required to minimize the differential column shortening are computational effort consuming, especially when considering various types of loads such as those listed above. Because the desired accuracy at this stage does not justify such luxury, two back propagation feed forward artificial neural networks (ANN) have been proposed in order to approximate these information. Instead of using a commercial software package, many references providing advanced principles have been considered to

code a program. The first designed ANN predicts the typical amount of time between two phases while performing sequential analysis, needed to achieve the minimum maximorum differential column shortening. The other aims to simulate sequential analysis results from those of simultaneous analysis. After the training phases, testing phases have been conducted in order to ensure the generalization ability of these respective systems. Numerical cases are studied to examine how good these ANN results match to the finite element method sequential analysis results. Comparison reveals an acceptable fit; enabling these systems to be safely used in the preliminary design stage.

Keywords: sequential analysis, substructure technique, computational resources, artificial neural network, differential column shortening, optimization.

ÖZ

Bu tez çalışması 3-boyutlu çerçevelerin yapım aşaması çözümlemesinin, yapısal bölümleme ile optimize edildiği bir analiz tekniğini içerir. Bu analiz modeli tüm yapının bir anda yüklenmesi yerine inşa edilme aşamalarına göre analizine dayanır. Gerçekci 3-boyutlu çerçevelere, kalıcı yerçekim yükü (ölü yük), değişken yerçekim yükleri (inşaat yükü, haraketli yük) ve diğer yükler ve etkiler (zamana bağlı, sıcaklık ve deprem) yapım aşamasına ve klasik yönteme göre uygulanmıştır. Bu analizlerin eğilme momenti ve tasarımdaki rolleri incelenerek karşılaştırılmıştır. Yapım aşaması analizinin uygulamasında optimizasyonu sağlamak için en uygun yapısal bölünme boyutu seçilmiştir. Böylece bigisayar çözümü için gerekli hafıza ve zaman minimize edilmiştir. Bu çalışmada sunulan örneklerle yapım aşaması analizinin önemi, daha doğru analiz sonuçları için gerekliliği, özellikle yüksek yapılarda öneminin daha da arttığı ispatlanmıştır.

Ancak 3-boyutlu çerçevelerin ön tasarımı safhasında optimum eleman boyutlarını ve göreceli kolon kısalmalarını minimize etmek, tekrarlanan yapım aşaması analizlerinde, yukarıdaki yükler de düşünüldüğünde oldukça güçtür. Bu sebeple bu aşamada kesin sonuçlara gereksinim duyulmaması sebebi ile yapay sinir ağları (YSA) ile çok yakın sonuçları verecek iki ağ geliştirilmiştir. Hazır bir paket program kullanmak yerine, birçok güncel yayın taranarak gelişmiş yöntemleri içerecek şekilde bir program hazırlanmıştır. Birinci yapay sinir ağı iki yapım aşaması arasında minimum maksimorum göreceli kolon kısalmasını verecek süreyi hesaplamaktadır. Diğer yapay sinir ağı ise klasik analiz sonuçlarından, yapım aşaması analiz sonuçlarını türetmektedir. İlk önce bu iki yapay zeka sisteminin parametreleri

saptanmıştır. Daha sonra bu parametre gurubunun doğru sonuçlar verip vermediği kontrol edilmiştir. Seçilen örneklerle yapay sinir ağları çözümlerinin sonlu elemanlar yapım aşaması çözümleriyle örtüştüğü ve ön tasarımda güvenlice kullanılabileceği ispatlanmıştır.

Anahtar Kelimeler: yapım aşaması analizi, yapısal bölümleme tekniği, işlem kaynakları, yapay sinir ağları, göreceli kolon kısalması, optimizasyon

To Paul, Florette, Yvan, Michelle,
Clarisse, and Benoit Sepkap

ACKNOWLEDGMENT

I would like to thank Asst. Prof. Dr Giray Özay for his continuous support and guidance in the preparation of this study. Without his invaluable supervision, all my efforts could have been short-sighted.

A singular thank goes to Prof. Dr Alagar Rangan for his permanent contributions, encouragements and support along all my studies. I am also obliged to Asst. Prof. Dr Alireza Rezaei, Asst. Prof. Dr. Serhan Şensoy, Asst. Prof. Dr Erdinç Soyer, Prof. Dr Özgür Eren, and Prof. Dr Marifi Güler for their assistance in different ways and at different stages during my thesis. In addition, numerous friends have always been assisting me in various ways. I would like to show them gratitude as well.

I owe quite a lot to my family who supported me in many manners all throughout my studies. I would like to express a deep gratitude to Cedric KOUAMOU W., my junior brother, for his helpful collaboration.

TABLE OF CONTENTS

LIST OF TABLES

LIST OF FIGURES

LIST OF SYMBOLS OR ABBREVIATIONS

Latin Characters

2D	two dimensional
3D	three dimensional
a_g	design ground acceleration for the return period
A	loaded area on a floor
A_0	= 10.0 m^2
ANN	artificial neural network method
CFM	correction factor method
CL	construction load
CPU	central processing unit
DL	dead load
e	accuracy of classification expected
$E_c(28)$	modulus of elasticity of concrete at 28 days
E_p	energy of a neural network system after the presentation of an arbitrary pattern
$error$	error at each output node after the presentation of the last epoch that corresponds to the end of the training phase
$f_{ck}(28)$	characteristic compressive strength of concrete at 28 days
f_{cm0}	= 10 MPa
$f_{cm}(28)$	mean of compressive strength at 28 days
f_e	yielding strength of steel
h	number of hidden units

K	stiffness matrix
LL	live load
lx	width of bays in X direction
ly	width of bays in Y direction
lz	height of stories
m	size of stiffness matrix; number of output units
m'	size of stiffness matrix
n	story number ($n > 2$) above the loaded structural elements of same category; number of input units
N-R	normal and rapid hardening
nx	number of bays in *X* direction
ny	number of bays in Y direction
nz	number of stories in the whole building
p	number of stories constituting the substructure
P	number of training patterns
P	load matrix
p_0	critical constant characterizing the number of stories constituting the substructure
R	number of columns at one floor level
R	range of building footprint size
R/C	reinforced concrete
RS	rapid hardening high strength
S	soil factor
$\mathbf{S}_b$	resultant boundary force matrix
$S_e(T)$	elastic response spectrum

SL	slowly hardening
SM-FEA	simultaneous analysis driven along finite element method
SQ-ANN	sequential analysis driven along artificial neural network method
SQ-FEA	sequential analysis driven along finite element method
SQ-STRU	sequential analysis driven along finite element method applied on the structure as a whole
SQ-SUBS	sequential analysis driven along finite element method applied on the structure regarded as a compilation of many substructures
t	age of concrete; target output value at a given output node; dummy variable
T	vibration period of a linear single-degree-of-freedom system
T_B	lower limit of the constant spectral acceleration branch
T_C	upper limit of the constant spectral acceleration branch
T_D	value defining the beginning of the constant displacement response range of the spectrum
TD	time dependent effect
TL	temperature load
t_s	age of concrete at the beginning of shrinkage
U	displacement matrix
v^*	positive constant
v_m	parameter of a neural network (weight or threshold)
W	energy of a neural network system after the presentation of an arbitrary pattern with the weight elimination technique
w_{ij}	weight from input unit i to hidden unit j
w_j	column of hidden unit j into the input-hidden weight matrix

x	natural input value at a given node
x'	preconditioned input value at a given node
x_{max}	maximum natural input value at a given node
x_{min}	minimum natural input value at a given node
y	actual output at a given output node; natural output value at a given node
y'	preconditioned output value at a given node
y_{max}	maximum natural output value at a given node
y_{min}	minimum natural output value at a given node

Greek Characters

α	momentum term
α_A	live load horizontal reduction factor
α_n	live load vertical reduction factor
α_T	coefficient of thermal expansion
β	scale factor
β_0	amplification factor of spectral acceleration for 5% viscous damping
η	damping correction; gain fraction or step size
λ	constant of small positive size
τ	counter of the learning process
ψ_0	coefficient as chosen from Annex A.1 of EN 1990

Subscripts

b	boundary

d	down boundary
i	interior
k	dummy variable
u	up boundary
s	dummy variable
t	dummy variable

Superscript

r	number of substructure

Chapter 1

INTRODUCTION

1.1 General Overview

Structural engineering calculations aim to choose, for a given structure, the suitable materials and to define its shapes and dimensions so that it could withstand safely all the loads applied on. To achieve this purpose, a correct investigation of all the actual loads and the way they are applied are very critical. Indeed, for any infrastructure, its erection is a gradual process: one part is constructed after another. So, loads are progressively generated, and their effects are thereby influenced.

However, as a general observation, structural engineers do not care about this concern. In fact, they used to consider the structure as a whole, account the possible loads applied on, and perform any of the available analyses. This happens because they are not generally aware of this method, and, moreover, very few computer program packages efficiently incorporate this feature. Therefore, they are accustomed to practice what is known as simultaneous analysis or straightforward analysis or conventional analysis (SM-FEA).

As it is presented above, the chronological setting up of different parts constituting a structure successively generates loads, which consecutively contribute to the stress development across the structure members. This sequential nature is accounted by a technique called sequential analysis or segmental analysis or stage construction analysis (SQ-FEA).

1.2 Literature Review

Few authors studied sequential analysis. Choi and Kim (1985) proposed a model based on this philosophy. They attempted to address the significance of SQ-FEA. By considering two 2D frames and just gravity loads applied on them, they compared the structural response from both analyses: SM-FEA and SQ-FEA. In addition, Kim and Shin (2011) took into account the effect of time dependence. Also, Kwak and Kim (2006) dealt with time dependent analysis of R/C frame structures considering construction sequence. They showed the importance of this aspect on differential column shortenings. Liu et al (2011), Azkune, Puente, and Insausti (2007), and Fu et al (2008) regarded the temperature effects. While addressing the problem of the control for super tall buildings during construction, Liu et al (2011) recommended that one should carefully consider time dependent effect, temperature, earthquake, and wind action.

Saffarini and Wilson (1983), as reported by Choi et al (1992), as well as Kim and Shin (2011) offered a method carried out from bottom to top. Choi and Kim (1985) proposed a method performed from top to bottom. As they recognized the high computational resources consummation of SQ-FEA, Choi et al (1992) as well as Kim and Shin (2011) attempted to lessen the required effort.

Kim and Shin (2011) focused their study on reducing the computing time for column shortening analysis. For this purpose, they considered that several building stories are lumped into one construction unit and are assumed to be constructed at a time. The Choi and Kim's model is processed, from top to bottom, by bunching many of the floors to form substructures. Notions of "active", "inactive" and "deactivated" are introduced. When a substructure is said to be active, its weight is considered to determine the deformation of both of the substructures below which is

said to be inactive, and the active substructure itself. So, the part of the structure above called deactivated, has been deformed in the previous stage of the analysis.

Although the aforementioned studies provided sound results, they did not give enough attention to some important aspects. Choi and Kim's model neglected the effects of the deformation that occurred in the inactive substructure due to its weight, in evaluating the behavior of the active substructure. The reverse way of this process, for example makes it difficult for any adaptation in case of change in the number of stories. Also, the substructuring model that Choi and Kim (1985) as well as Kim and Shin (2011) proposed assumes the entire substructure to be constructed at a time, a fact that reduces the accuracy of the analysis.

Surprisingly, along their models, none of these studies states, clearly, how to size the substructure or the lumps. They aimed to trim down separately either the size of equations or the needed time, but never both in the same process. Among those who address the contribution of elementary loads, none considered many of them together in order to show the influence of one load to another's effect; and none accounted the respective effect of construction load, live load and earthquake.

Anyway, all of them and other authors agreed that the differences between the two analyses are due to the: (1) differential column shortening (Choi and Kim, 1985); (2) sequential application of dead load (Choi and Kim, 1985; Fu et al, 2008; Ozay and Njomo, 2012a), and temperature actions (Fu et al, 2008; Ozay and Njomo, 2012a; Azkune, Puente, and Insausti, 2007); (3) aging, creep, and shrinkage of the concrete (Kwak and Kim, 2006; Fu et al, 2008; Ozay and Njomo, 2012a); and (4) consideration of the coming and going of construction loads (Fu et al, 2008; Ozay and Njomo, 2012a).

Differential column shortening may affect non structural elements (Fintel, Ghosh, and Iyengar, 1986), aesthetic appearance, and the normal use of edifices. To decrease its effects, Fintel, Ghosh and Iyengar (1986) developed a compensation method. Herein, for the same goal, a minimization model has been proposed. Given a structure destined to some use, made in a definite-characteristic material and located in a particular environment, the structural response depends on the timing of the construction sequence. Thus, the amount of the differential shortening is function of the interphase, i.e. the typical duration between two consecutive stages.

On the other hand, considering all actions and trying to reduce the effect of differential column shortening while performing SQ-FEA calls for much more computational effort than SM-FEA since it requires many intermediate computations in addition to the final stage analysis that “corresponds” to the simultaneous analysis. But regarding the accuracy and the features carried by this strategy, this excess demand is justified, though it needs to be lowered. Some research works tried to accomplish this purpose by getting SQ-FEA’s results from those of SM-FEA.

Choi et al (1992) proposed the so called correction factor method (CFM) based on regression analysis. They claimed to well approximate SQ-FEA’s results considering only dead loads on 2D frames. Gupta and Sharma (2001) reported that Khan (1997) developed a neural network which simulates results of SQ-FEA from those of one stage analysis. They accounted that the neural net did not take into account the time dependent effect. These models are not realistic since they do not depict the actual situation of edifices: buildings are neither bi-dimensional nor protected against time dependent effects which contribute among others to the differential movement, but they are, in addition to dead loads, submitted under many other actions.

Even though, the seriousness of these studies has been recognized among the scientific community, the gap as presented above is still present. Moreover, the regression analysis used by Choi et al may suffer from constraints such as the linear or curvilinear relationship of the data with heteroscedatic error (Walczak and Cerpa, 1999). Khan (1997) tried to overcome this limitation with a multilayer feedforward neural network. He took profit to the fact that this system is a universal function approximator that can interpolate between vectors (Gupta and Sharma, 2011; Walczak and Cerpa, 1999; Belic I, 2012, pp. 3-22; Leondes, 1998; Iliadis and Jayne C, 2011; Fausett L, 1994; Haykin, 2005).

Nevertheless, it is capital to provide a tool to reduce the computational effort needed to obtain near accurate results as well as to determine the sequence's interphase with the intention to be able to make good decision in the earlier stage of preliminary study (Gupta and Sharma, 2011); since it is the project phase that is the most influential in the total cost (Haroglu et al, 2009; Ballal and Sher, 2003). In the present thesis, the soft computing tool artificial neural network is held to take down the computational effort and the differential column shortening on R/C 3D frame. Various types of loads are considered. These include dead loads, time dependent effects, temperature actions, construction forces and live load. Seismic loads are not considered here since they induce similar structural response whether considering sequential analysis or simultaneous analysis (Ozay and Njomo, 2012a).

1.3 Objectives of the Study

Different goals drove this study. In general, all tried to promote the sequential analysis while reducing the computational effort it requires.

a. The first goal accounted various loads sequentially applied and investigated their actual respective contribution. By this way, it expected to exhibit the significance of the SQ-FEA.

b. The second goal was to reduce the computational resources required to perform sequential analysis.

c. The third goal determined the optimal duration between two phases, yielding to a minimum differential column shortening.

d. The fourth goal predicted the sequential analysis results from those of simultaneous ones.

1.4 Reasons for Objectives

The convergence of these goals contributes to bridge from the SM-FEA to the SQ-FEA with less effort.

a. Isolating the individual contribution of a particular load points out the difference of sequential analysis versus simultaneous analysis. It may also be helpful to decide whether it is enough to consider simultaneous analysis for some loading cases or not. Anyway, the significance of SQ-FEA is underscored.

b. Sequential analysis consists in performing analyses at various stages and requires storing information for the next stage. As a result, it is needed a lot of CPU memory and a large amount of computational time. Nowadays, the demand of efficient algorithm is competitively growing. Although many computers are much performing than ever, the increasing complexity of buildings may make them unable to solve some problems if the algorithm is not carefully studied.

c. Differential column shortening has a negative effect at various points of a project: it affect the aesthetical aspect, the normal functionality of the infrastructure, and even the non structural elements. So, it is a great advantage to economically and environment-friendly reduce this facet by just fine-tuning the construction timing.

d. At earlier stage of a project study, namely preliminary design phase where the optimal structural systems are looked for, it is a profligacy to complete the repeated SQ-FEAs with results of 100% accuracy. Instead, a workaround may consist in carrying out the SM-FEA, and approximate from their results those for SQ-FEA.

1.5 Work Done to Achieve Objectives

The different goals targeted herein have been overcome by finite element analysis followed by either statistical model or artificial neural network tool.

a. A realistic R/C 3D frame representing a middle-rise building, an everyday's situation, has been submitted under various loading cases. The structural responses from both simultaneous and sequential analysis have been peeled off and the isolated effect of each loading case from one analysis has been compared with its corresponding version from the other analysis.

b. To reduce the computational resources needed, the sequential analysis has been coupled with the substructure technique. Finite element analysis has been applied on several numerical cases, and a statistical model has been drawn to optimize the obtained merger (SQ-SUBS).

c. Many buildings ranging throughout the practical interval have been analyzed with the finite element method through the sequential scheme. For each one, the result was the optimal duration yielding to minimal differential column

shortening. A neural network has been trained to simulate the relationship between the building characteristics and the optimal duration.

d. As in the previous point, the same buildings, analyzed with SQ-FEA, provided vectors to develop an ANN. It aims to approximate the SQ-FEA results from those of SM-FEA in order to get SQ-ANN.

1.6 Achievements

In general, all the objectives contribute to emphasize on the importance of the sequential analysis while proposing efficient algorithms or practical tools to reduce the computational effort it requires, with the intention to contribute to the implementation of proficient software packages.

a. By investigating the contributions of different loading cases, it appeared that some of them are kept almost the same whether SQ-FEA or SM-FEA. On the other side, some happened to be very sensitive to SQ-FEA. This information has been revealed to be important when these latter loads are predominant in a project or may be useful to decide whether to conduct SQ-FEA or not. Overall, the significance of SQ-FEA over the SM-FEA has been highlighted since the final combined structural response has been too divergent.

b. The statistical model designed from the results of many building analyses ended to an optimized merger: a substructure sizing method has been developed with the intention to minimize the CPU memory and the time needed to SQ-SUBS computations. The implication of the substructure technique will not influence the analysis accuracy.

c. Given any R/C 3D frame determined by obvious properties like the number of stories or the ambient temperature change, an ANN has be trained to predict

which construction duration between two stories would minimize the maximal differential column shortening.

d. A simple method based on ANN tool, intending to approximately deduct SQ-FEA results from those of SM-FEA has been trained; this happens to be very helpful for example during the phase of preliminary design when the accuracy provided by the repeated and resource consuming SQ-FEA is a luxury. The SQ-ANN's results showed that ANNs are good tools to settle this fastidious problem.

1.7 Thesis's Outline

This thesis is made of five other chapters. All of them convey to achieve the points mentioned above. In the following chapter, all the different loads involved in this study have been assessed: dead load, live load, time dependent effects, temperature action, and earthquake. Their values have been adopted along the respective code prescriptions.

Then, in the third chapter, the sequential analysis theory is stated. The issue of column differential shortening is clearly studied here. Furthermore, the respective contribution of each loading type has been evaluated in the SQ-FEA versus SM-FEA. The result has been to emphasize the significance of the sequential method.

Chapter 4 recalled the substructure technique, and coupled this technique with the SQ-FEA. The aim of this part (SQ-SUBS) has been to shorten the computational resources required for SQ-STRU. Numerical cases have been considered to illustrate the results.

After that, the theory about the soft computing neural network has been reported in the fifth chapter. Many references have been considered in order to facilitate its implementation. Plus, this chapter dealt with the acute problematic of approaching

the sequential results in the design stage. Two artificial neural networks have been developed to estimate the step duration yielding to minimum maximorum differential shortening on the one hand, and, on the other, to approximate SQ-FEA's results from those of simultaneous one.

Finally, Chapter 6 ends the present thesis. It has been devoted to the general summary of the current work. Recommendations and further works have been also proposed.

Chapter 2

REVIEW OF COMMON LOADS APPLIED ON BUILDINGS

Many criteria can be used to classify loads applied on buildings. One can choose to distinguish mechanical loads (dead load, live load, construction load, wind action and earthquake) from non- mechanical ones (time dependent effect and temperature). Some may opt to differentiate gravity loads (dead load, live load, and construction load) versus non-gravity ones (time dependent effect, temperature, wind action and earthquake); or others, to separate lateral loads (wind action and earthquake) from non-lateral ones (dead load, live load, construction load, time dependent effect, and temperature). This last classification system has been the concern of the present work. Herein, all the non-lateral loads have been considered, but the wind action has been neglected compared to the earthquake effect.

Because of the location of the numerical cases and their availability in software packages, the current study has been based on:

- *Eurocode 1 : « Bases de Calculs et Actions sur les Structures et Documents d'Application Nationale*, » for estimations of dead load, live load, construction load, and temperature action;
- *Eurocode 8 : « Conception et dimensionnement des structures pour leur résistance aux séismes et documents d'application nationale »*, plus "*A review of the seismic hazard zonation in national building codes in the context of Eurocode 8"* for all computations related to earthquake, and;

- CEB-FIP Model Code 1990, for handling the material properties such as thermal expansion, strength and time dependent effects.

2.1 Dead Load

Following Article 5.2.1 of Part 1-1 within the Eurocode 1, the characteristic values of self weight, dimensions and specific weight have been determined accordingly to Article 4.1.2 (1) of EN 1990. Actually, Annex A of Part 1-1 recalls the specific weight of many materials. Table 2.1 displays an excerpt related to concrete.

Table 2.1. Specific weight of some materials

Material	Specific weight (kN/m^3)
Light Concrete	
Specific mass class LC 1.0	9.0 to 10.0[1,2]
Specific mass class LC 1.2	10.0 to 12.0[1,2]
Specific mass class LC 1.4	12.0 to 14.0[1,2]
Specific mass class LC 1.6	14.0 to 16.0[1,2]
Specific mass class LC 1.8	16.0 to 18.0[1,2]
Specific mass class LC 2.0	18.0 to 20.0[1,2]
Normal weight concrete	24.0[1,2]
Heavy concrete	>[1,2]

[1] Increase by 1 kN/m^3 in case of normal reinforcement rate in reinforced concrete or prestressed concrete

[2] Increase by 1 kN/m^3 in case of soft concrete

From there, the specific weight of the reinforced concrete has been fixed as 25 kN/m^3. Article 5.2.2 (2) adds: the light partitions' self weight should be considered as distributed loads that have to be included in the live loads.

Table 2.2. Building classification and corresponding live loads

Category	Explanation / details		Live load (kN/m^2)
A **Domestic, residential**	Local in residential buildings/houses; rooms in hospitals.	**Slabs**	1.5 to 2.0
		Stairs	2.0 to 4.0
	Hotels/motels rooms; kitchen and sanitary room	**Balconies**	2.5 to 4.0
B **Offices**			2.0 to 3.0
C **Meeting spaces (except surfaces from categories A, B and D)**	**C1**: spaces with tables		2.0 to 3.0
	C2: spaces with fixed seats		3.0 to 4.0
	C3: spaces with free circulation of people		3.0 to 5.0
	C4: spaces allowing physical exercises		4.5 to 5.0
	C5: spaces likely to be crowded		5.0 to 7.5
D **Commerce**	**D1**: normal retail trade		4.0 to 5.0
	D2: supermarkets		4.0 to 5.0

2.2 Live Load

For live loads, buildings are classified into four main categories. Table 2.2 reports the different categories and the corresponding loads, as stipulated in Article 6.3.1. Paragraph 6.3.1.2 (8) specifies the light partitions' self weight to be added to live load as follows:

- light partitions' self weight ≤ 1.0 kN per meter of wall 0.5 kN/m^2;
- light partitions' self weight ≤ 2.0 kN per meter of wall 0.8 kN/m^2;
- light partitions' self weight ≤ 3.0 kN per meter of wall 1.2 kN/m^2.

Paragraph 6.3.1.2 (9) concerns the heavy partitions. Paragraph 6.3.1.2 (10) and Paragraph 6.3.1.2 (11) deals with the horizontal and vertical reduction factor. The horizontal reduction factor α_A is determined as follows:

$$\alpha_A = \min(\frac{5}{7}\ \psi_0 + \frac{A_0}{A}; 1.0) \quad (2.1)$$

with $\alpha_A \geq 0.6$ for categories C and D, and where

ψ_0 is the coefficient as chosen from Annex A.1 of EN 1990. $\psi_0 = 0.7$ for the categories discussed above;

A_0 = 10.0 m^2;

A is the loaded area.

For the vertical reduction factor α_n, it is obtained by:

$$\alpha_n = \frac{2+(n-2)\psi_0}{n} \quad (2.2)$$

where n is the story number ($n > 2$) above the loaded structural elements of same category.

Herein, these recommendations have been simplified and an overall value for live load has been adopted. Also, the roof has been considered with the same use as the other floor. Anyway, these simplifications do not reduce the seriousness of the targeted goal, but just alleviate the calculation process for a better comprehension.

2.3 Construction Loads

Part 2-6 gives an interest on action during work execution. It includes amongst other loads, the construction loads which are defined as loads other than environmental and climatic in nature, and which have to be considered in the design during the construction process. Article 4.8.1 (2) stipulates that it is suitable to these actions to be evaluated accordingly to the project's specifications.

2.4 Temperature Action

The temperature action matter is provided by Part 2-5. Article 5.1.3 (3) authorizes to suppose a uniform temperature distribution for common buildings where the computations are required. It adds that national maps showing isotherms of temperature from Stevenson screen can be used.

Article 2.1.8.3 of CEB-FIP Model Code 1990 proposes to take the coefficient of thermal expansion as $\alpha_T = 10 \times 10^{-6}\, K^{-1}$ for structural analysis. It must be noted that the temperature dependence of materials has not been accounted in the scope of this study.

2.5 Time dependent Effect

The main source discussing about time dependent effects is CEB-FIP Model Code 1990. This code provides formulas to predict the characteristics of R/C along the time. Compressive strength, tensile strength, modulus of elasticity, creep, and shrinkage have been all concerned herein.

2.5.1 Compressive Strength

Once the specific characteristic compressive strength or the mean value of compressive strength at 28 days has been chosen, Article 2.3.1.2 and Article 2.1.6.1 detail how to find the compressive strength of concrete at age t days depending on the type of cement used in the mixture. In this procedure, the coefficient s expressing the type of cement is valued in Table 2.3.

Table 2.3. Time dependent cement parameters

Cement type		**RS**	**N-R**	**SL**
	s	0.20	0.25	0.38
creep	α	1	0	-1
Shrinkage	β	8	5	4

RS: Rapid Hardening high strength. **N-R**: Normal and rapid hardening. **SL**: slowly hardening.

2.5.2 Tensile Strength

The tensile strength is firmly dependent on the specific characteristic compressive strength according to Article 2.1.3.3.1.

2.5.3 Modulus of Elasticity

Article 2.1.4.2 gives the value of the modulus of elasticity at 28 days from the mean of compressive strength at $t = 28\,days$. It states that $E_c(28) = 21500\,[\frac{f_{cm}(28)}{f_{cm0}}]^{\frac{1}{3}}$ with $f_{cm0} = 10\,MPa$. The modulus of elasticity of concrete at any date may be predicted from that at 28 days and the type of cement, as described in Article 2.1.6.3; thus it is also dependent on the mean of compressive strength at 28 days.

2.5.4 Creep

Expressed in terms of creep compliance or creep function, the creep is treated in Article 2.1.6.4.3. It is related to the creep coefficient, the modulus of elasticity at 28 days, and the modulus of elasticity at the loading age which is also dependent of that at 28 days as seen in section 2.5.3 of the present thesis. The creep coefficient is a product of two quantities: the notional creep coefficient and a time dependent coefficient describing the creep development after loading. These two quantities vary in respect of the relative humidity of the ambient environment, the member's cross section dimensions, and the age of the concrete at the loading. In addition, the former changes with the variation of the mean value of compressive strength at 28 days, as well.

2.5.5 Shrinkage or Swelling

The total shrinkage/swelling strains at t days are concerned in Article 2.1.6.4.4. It may be obtained from two parameters. The first is the notional shrinkage coefficient which may be calculated from the relative humidity of the ambient environment, the

mean of compressive strength at 28 days, and a cement dependent shrinkage coefficient from Table 2.3. On the other hand, the second parameter is a time dependent coefficient describing the shrinkage/swelling development. It is a function of the age of concrete at the beginning of shrinkage/swelling and the cross sectional geometry of the structural member.

In conclusion, the non-lateral forces as described above are mainly dependent on:

- the specific weight of the constituting material (which is constant for R/C);
- the member's cross section dimensions;
- the member's lengths;
- the whole structure's geometry;
- the use of the edifice;
- the external temperature;
- the type of cement used in concrete mixture;
- the mean value of compressive strength at 28 days;
- the relative humidity of the ambient environment;
- the age of the concrete at the loading;
- the age of the concrete at the beginning of the shrinkage/swelling.

These few parameters can be said to be determinant in the assessment of the non-lateral loads applied on an R/C 3D frame structure, and, thus, in the prediction of its structural response with respect to these loads.

2.6 Earthquake

2.6.1 Seismicity Zone

Analyses to withstand against earthquake are fundamentally dependent on seismic hazard. Locations are divided into different seismic hazard levels within each country. In particular, Prof C. Chrysostomou prepared a personal communication

including a recent code revision (2004), as reported by Solomos, Pinto, and Dimova (2008), in which he allocated for each seismic hazard zone, a peak ground acceleration in Cyprus. Figure 2.1 below depicts this seismic zonation.

Figure 2.1. Seismic zonation map of Cyprus.

2.6.2 Class of Soil

This seismic zonation has been proposed for a stiff soil or rock, so the actual nature of the building location has to be considered. The geological nature of the site is of a great importance; it may contribute to accelerate or to decelerate waves traveling through its layers, and, thus, influences the impact of the earthquake on edifices. Part 1.1 of Eurocode 8 in its Article 3.2 distinguishes three classes of site. Table 2.4 described potential soils one can find in a given site as well as the shear-wave velocity in the upper 30 m. In addition, it should be noted that Article 3.2 (2) points out that complements or modifications can be added to this classification in order to take into account particular soil conditions.

Table 2.4. Site classification

Site class	Description	shear-wave velocity
A	Rock or other rock-like geological formation, including at most 5 m of weaker material at the surface	>800 m/s
	Deposits of very dense sand, gravel, or very stiff clay, at least several tens of meters in thickness and characterized by a gradual increase of mechanical properties with depth	>400 m/s
B	Deep deposits of dense or medium-dense sand, gravel, or stiff clay with thicknesses from several tens to many hundreds of meters	200 – 350 m/s
C	Deposits of loose-to-medium non-cohesive soil (with or without some soft cohesive layers)	< 200 m/s
	Deposits consisting of predominantly soft-to-firm cohesive soil	< 200 m/s

2.6.3 Importance of the Building

According to the expected damage that could allow the immediate use or the collapse of edifices, Part 1.2 in its Article 3.7 separates buildings in importance classes, allocating to each a coefficient said to be of importance. Table 2.5 recapitulates this classification.

Table 2.5. Importance classes of Buildings

Class	Description	Coeff.
I	Buildings whose integrity during earthquakes is of vital importance for civil protection (hospitals, fire stations, power plants, …)	1.4
II	Building whose seismic resistance is of importance in view of the consequences associated with a collapse (schools, assembly halls, cultural institutions, …)	1.2
III	Ordinary buildings, not belonging in the other categories	1.0
IV	Buildings of minor importance for public safety (agricultural buildings, …)	0.8

2.6.4 Live Load Contribution

To consider the probability that the live load may not fully be present at the instant an earthquake occurs, coefficients fixing the contribution of the live load are available. Also, they account the partial participation to the structure's motion of non-firmly fixed masses. It is given below in Table 2.6 for the common buildings as studied in Section 2.1 of the present thesis, as specified in Article 3.6 of Part 1.2.

2.6.5 Seismic Action

Eurocode 8 distinguishes various representations of the seismic action. In Part 1.1, Article 4.2.1 (2) recommends to use the elastic response spectrum; unless, particular studies specify otherwise. Through the elastic response spectrum, the two horizontal components of the seismic action are defined with respect of vibration period. Figure 2.2 depicts this definition. Formulas are provided to characterize each part of the curve. Table 2.7 completes the formulas by supplying their parameters' values.

Table 2.6. Live load participation factor

Purpose of the building	**Factor**
Category A: domestic, residential	0.30
Category B: offices	0.30
Category C: meeting halls	0.60
Category E: depots, warehouse	0.80

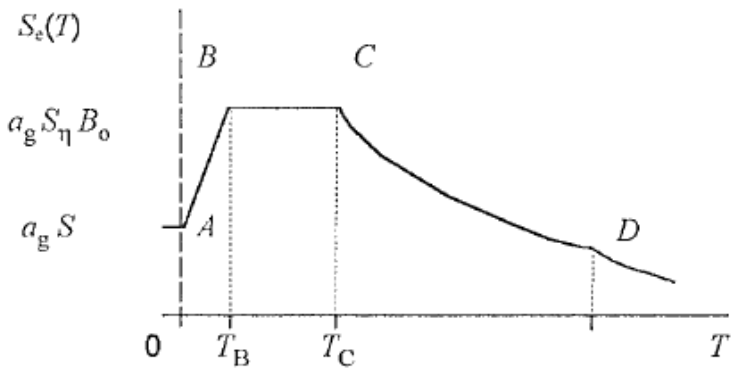

Figure 2.2. Representation of the elastic response spectrum.

The elastic response spectrum $S_e(T)$ for the return period is defined as follows:

$$S_e(T) = \begin{cases} a_g \cdot S \cdot \left[1 + \frac{T}{T_B}(\eta \cdot \beta_0 - 1)\right], \ 0 \le T \le T_B \\ a_g \cdot S \cdot \eta \cdot \beta_0, \ T_B \le T \le T_C \\ a_g \cdot S \cdot \eta \cdot \beta_0 \cdot \left[\frac{T_C}{T}\right]^{k_1}, \ T_C \le T \le T_D \\ a_g \cdot S \cdot \eta \cdot \beta_0 \cdot \left[\frac{T_C}{T_D}\right]^{k_1} \cdot \left[\frac{T_D}{T}\right]^{k_2}, \ T \le T_D \end{cases}; \quad (2.3)$$

where:

$S_e(T)$ elastic response spectrum;

T vibration period of a linear single-degree-of-freedom system;

a_g design ground acceleration for the return period;

β_0 amplification factor of spectral acceleration for 5% viscous damping;

T_B, T_C limits of the constant spectral acceleration branch;

T_D value defining the beginning of the constant displacement response range of the spectrum;

S soil factor;

η damping correction factor – its reference value is $\eta=1$ for 5% viscous damping.

Table 2.7. Values of elastic response spectrum's parameters

Site class	S	β_0	k_1	k_2	T_B (s)	T_C (s)	T_D (s)
A	1.0	2.5	1.0	2.0	0.10	0.4	3.0
B	1.0	2.5	1.0	2.0	0.15	0.6	3.0
C	0.9	2.5	1.0	2.0	0.20	0.8	3.0

Chapter 3

SEQUENTIAL ANALYSIS: THEORY AND SIGNIFICANCE

Choi and Kim (1985) described a strategy to perform SQ-FEA. However, it is maculated of some limitations affecting the result accuracy. Plus, since the authors regarded only dead load, the strategy does not point how to include the other loading types. The following paragraphs propose a sequential analysis strategy modeled on the construction process; it accounts various loads: dead load, live load, construction load, time dependent effect, temperature, and earthquake. The proposed model leads to more realistic results.

3.1 Proposed Sequential Analysis Strategy

Sequential analysis of a given building consists of successive analyses at different dates along the construction process. The typical schedule considered herein is to set each story erection as a phase. At the beginning, the first story is erected and put over formwork. The new cast structure is left for a definite period, termed as interphase, while getting hard. During this elapsing period, it undergoes temperature stresses and time dependent effects. An analysis is conducted in order to determine the structural response at the end of this stage. It shows that this part of the structure has performed deformations and presents internal forces across its members.

After that, the story is stricken and the second floor is constructed over shores supported by the existing slab. Instead of keeping the idealized length of column in this new floor, the top is leveled at the designed position. From this moment and

during the interphase, the first floor supports its own dead load, the construction loads from the second floor, temperature action and time dependent effects; and the second floor is submitted under temperature stresses and time dependent effects. Once more, a second analysis is completed considering the deformed shape of the existing structure as reference. This new analysis regards the first story as weightless since its weight has been already considered in the first analysis, but it takes into account the temperature action and the time dependent effect occurred during the last interphase. The analysis reveals a new structural response which is cumulated to the previous one.

At the end of the second period, the third floor comes; and the part of the structure, constituted by the first and the second stories serves altogether as the first one, while the third as the second of the preceding phase. Here, the construction loads formerly applied on the first slab is removed. Operations are repeated till the last floor which is not subjected to any construction load, but to the all remaining load types. After an appropriate analysis, like finite element method for example, has been performed and structural response summed up, the live load is applied along with temperature action and time dependent effect considering the deformed geometry as reference.

In this thesis, for non-lateral loads, even if the deformed shape has been accounted for the elastic stiffness, displacements and deformations have been assumed to be relatively small so that the equilibrium equations could be stated using the idealized shape and the geometric stiffness matrix could be neglected. However, this aspect has been considered when the displacements became large, for example in the case of earthquake, as prescribed by Przemieniecki (1968).

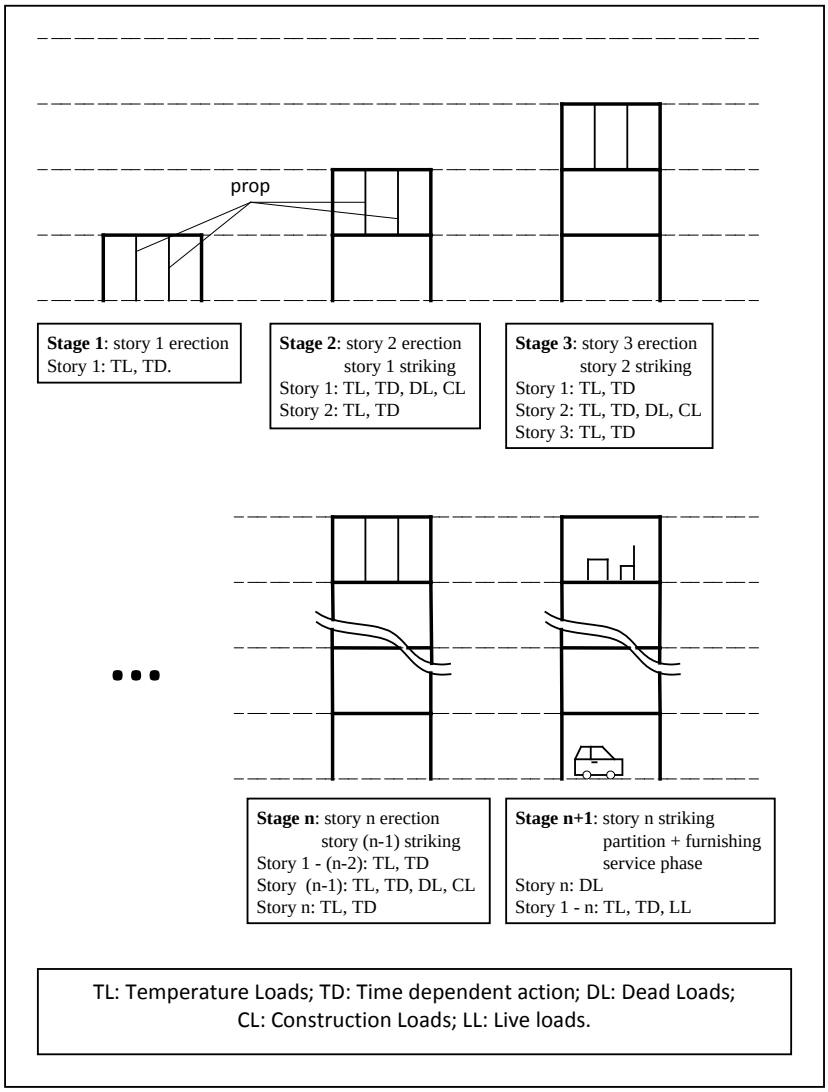

Figure 3.1. Sequential analysis process.

3.2 Significance of Sequential Analysis

It has been underlined that many projects are still being studied through a straightforward elastic linear analysis. The studies mentioned above tried to warn against this habit. Indeed, the results obtained from the straightforward analysis are so different from the reality. Therefore, the value of the sequential method regarding bending moments on 3D-frame members under common sequential loading effects which are self weight, creep, shrinkage, temperature, construction loads, and then other types of loads as earthquake after furnishing + functional live loads, should be emphasized.

3.2.1 Case Definition

For this purpose, an L-shaped 15-story office building has been analyzed using the commercial computer program SAP2000 version 15.1.0. Figure 3.2 represents its plan configuration and its members' dimensions are recapitulated as in Table 3.1. Slabs are of 120 mm in thickness. These structural elements are made of reinforced concrete whose compressive strength at 28 days is $f_{cm}(28) = 20\,MPa$ and the desired elastic modulus $E_c(28) = 21\,GPa$. The concrete is assumed to be very well mixed so that the standard deviation of the set of sample compressive strengths is very small; therefore, $f_{ck}(28) \cong f_{cm}(28)$. The yielding strength of steel is $f_e = 415\,MPa$. The concrete is prepared with a normal hardening cement and the shrinkage starts at $t_s = 0\,day$.

The local site is located in Famagusta, North Cyprus, on site class B with a type 2 spectrum. The site relative humidity is taken as 61.6%. The temperature change through the construction process is adopted as -15°C which is assumed to be linear from the beginning point to final one. 2.0 kN/m^2 value is used for office live load including light weight partition walls. 30% of this live load contribute to the earthquake analysis. Construction loads are assumed to be the weight of the shored floor increased by 20% to consider work loadings and formwork weight. Table 3.2 shows the construction schedule.

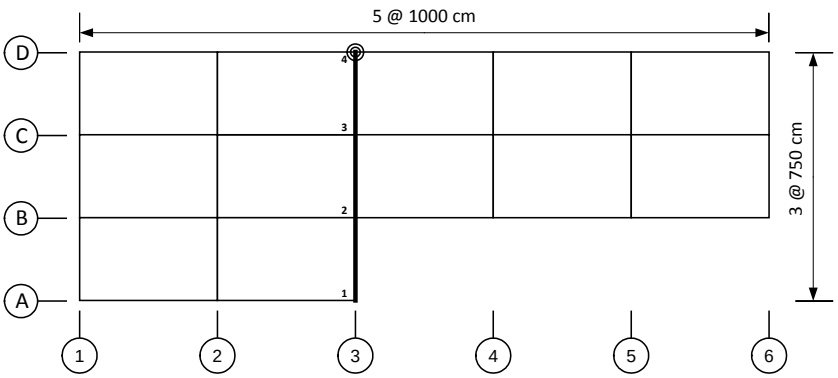

Figure 3.2. Plan configuration of the 15-story building.

Table 3.1. Dimensions of 3D-frame members in reinforced concrete

Floor	Member	Width × Depth (cm)	Cross area of concrete (cm^2)
1-15	Beam	25 × 60	1500
10-15	Column	30 × 60	1800
7-10		40 × 60	2400
1-6		60 × 60	3600

Table 3.2. Construction sequence

Stage	Duration (in days)	Added Structure	Operations
1	10	Story 1	
2	10	Story 2	Striking story 1
3	10	Story 3	Striking story 2
4	10	Story 4	Striking story 3
5	10	Story 5	Striking story 4
6	10	Story 6	Striking story 5
7	10	Story 7	Striking story 6
8	10	Story 8	Striking story 7
9	10	Story 9	Striking story 8
10	10	Story 10	Striking story 9
11	10	Story 11	Striking story 10
12	10	Story 12	Striking story 11
13	10	Story 13	Striking story 12
14	10	Story 14	Striking story 13
15	10	Story 15	Striking story 14
16	10		Striking story 15; partition and furnishing; service phase

3.2.2 Results and Discussions

Once SQ-FEA and SM-FEA have been performed, attention has been given on the frame 3 in Figure 3.2. Moments have been regarded along the beams of the 1^{st}, the 5^{th}, the 10^{th} and the 15^{th} story, as well as both but separately, at the top and bottom of each column of the chain 3D encircled in the figure. These quantities are compared in terms of differences given as percentage of the corresponding bending moments obtained from straightforward analysis, taken as reference.

Figure 3.3 presents the bending moments along the selected beams. The following inferences can be made from the figure:

- The two analyses yield to much bunchy moments in the lower floors than in the upper ones where a difference of 62% has been observed. This confirms the fact, reported by Choi and Kim (1985) and Kwak and Kim (2006), that the sequential analysis is more important for tall buildings.
- Sequential analysis tends to reduce the difference of moments from one side to another of the intermediate columns. At the second support of the 15th story beam, SQ-FEA shows a moment difference of 7% from one side to another and SM-FEA a difference of 41%. By reducing this difference, the column behaves safer and does not require so much reinforcement. Also, the reinforcement applied for superior layer in one side of the beam can be extended to the other side without major losses for practical convenience.
- The span with irregularity (the first one) exhibits more difference than the spans with regularities. This result may also be extended for the global case of a whole building: irregular edifices are more sensitive to the difference SQ-FEA versus SM-FEA than regular ones.
- The live loads, applied at a time for both analyses, reduce the divergence between them. For example, the difference changes from 80% to 62% at the first support of the upper beam.

Figure 3.4 reveals the bending moments' variation along a column. It shows the contribution on final moments for all the loading effects involved. These effects go from dead load (DL) to live load (LL) through creep and shrinkage (TD), construction load (CL) and temperature load (TL). It shows that:

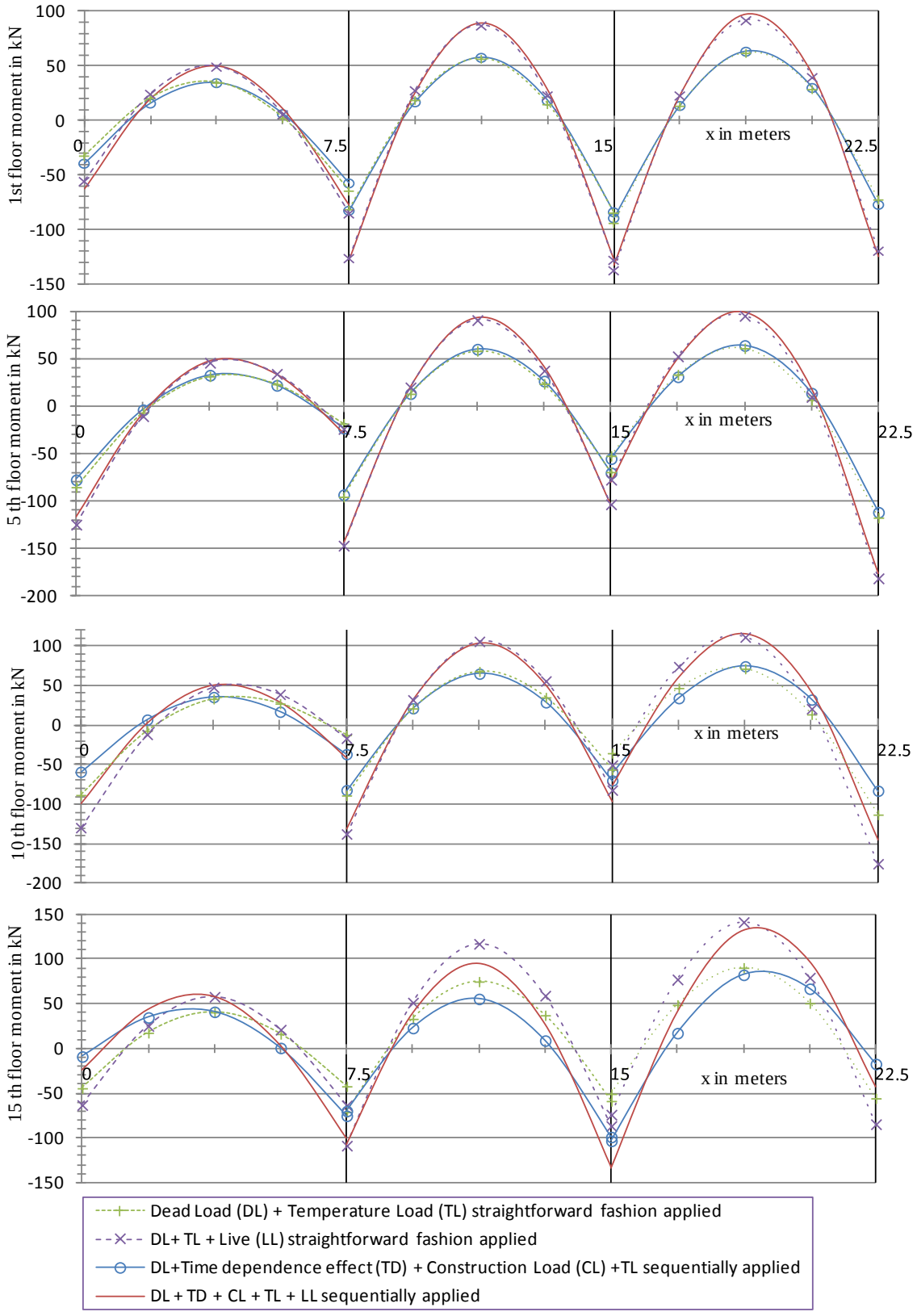

Figure 3.3. Bending moments along the beams of 1st, 5th, 10th and 15th floor.

i) Top Moment

- The time dependent effect causes a change varying from -20% to +20%.
- The consideration of construction loads is significant since it generates a moment variation from -14% to 10%.
- These two previous effects act more significantly at the extremities of the whole structure.
- The temperature does not have a major effect except in the lower floors where it may reduce the response of the structure by 50% for sequential analysis and completely inverse the sign of the moment for straightforward analysis from -65.36 kNm to +14.49 kNm. Temperature applied at a time causes more structural response than considering it applied sequentially;
- The shape of the final moment curve is dictated by the curve when temperature is considered.
- The live load tends to reduce the difference between the two analyses. A change from 50.7% to 35.6% can be noticed.
- Above floor 5, the straightforward analysis yields to redundant internal forces, up to 35.6%.
- But, below floor 5, it yields to unsafe results varying from -1.2% to -76.3% difference.

ii) Bottom Moment

- The time dependent moment's curve seems to keep a progressive variation with +23.5% change at floor 1, -18.7% at floor 2 to - 33.6% at floor 15.

- Similarly, the construction load moment curve keeps the same progressive variation along the structure height with +9.5% at floor 1, -13.8% at floor 2 to -32.6% at floor 15.
- The temperature load is insignificant in the upper stories but causes +49.3% change in the 2nd story and inverse the sign of the moment in the 1st floor, from +35.62 kNm to -15.43 kNm for sequential analysis. Also here, sequential temperature stresses the structure less than temperature applied at the time.
- The shape of the final curve is once more dictated by the curve when considering temperature.
- The sequential analysis yields to more economical results for up to 98.7 %.

The same structure is also analyzed under the earthquake with two initial shapes: first, considering the un-deformed shape of the total structure; and second, after the deformation happened due to previous loads. The mass centers of these two initial shapes form the vector (0.7 mm, 0.1 mm, -7.6 mm) whose length is 7.7 mm. The moments obtained from these analyses are not significantly divergent. This mass center translation and the overall deformation of the structure after sequential analysis are insignificant regarding the effect of the earthquake. Figure 3.5 explains the resulting moments.

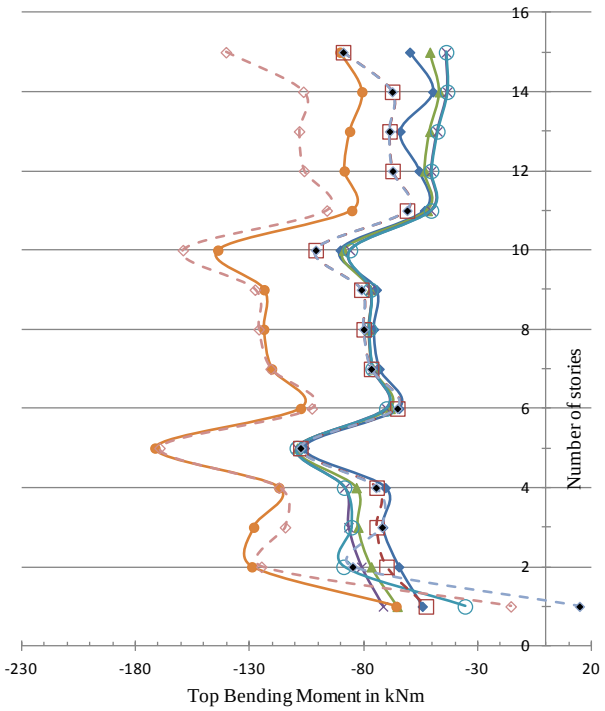

(a)

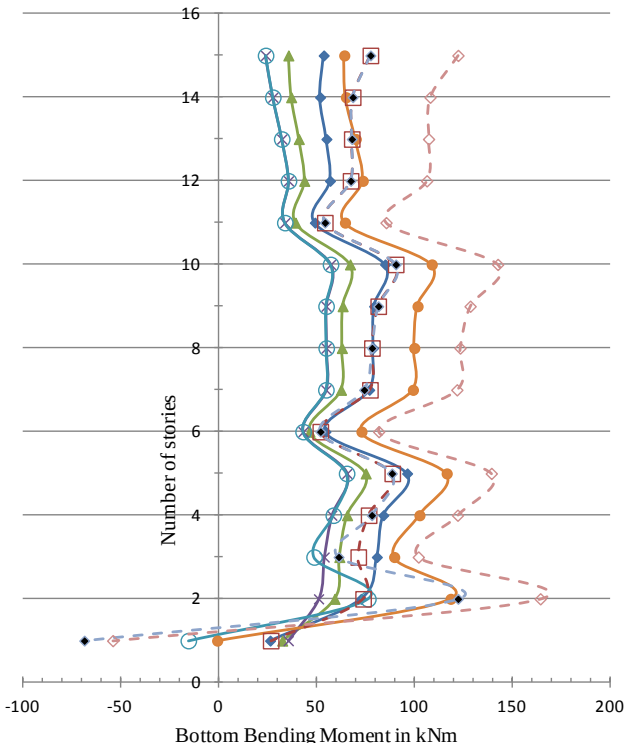

(b)

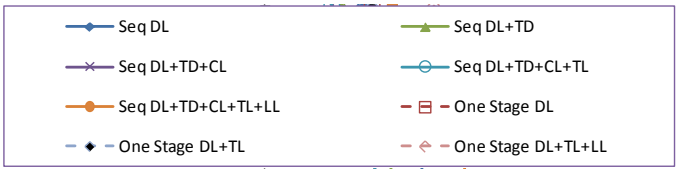

Figure 3.4. Bending moments along the column 3D. (a) Top node. (b) Bottom node.

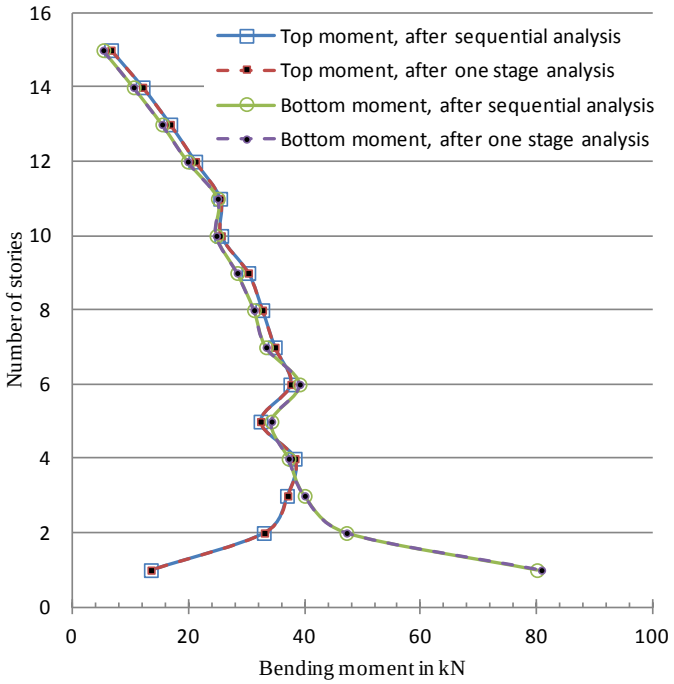

Figure 3.5. Bending moments obtained from earthquake analysis.

Chapter 4

SEQUENTIAL ANALYSIS: SUBSTRUCTURING AND OPTIMIZATION

Although Choi and Kim (1985) as well as Kim and Shin (2011) ingeniously attempted to merged SQ-FEA with substructuring technique with the intention to lessen the effort required to conduct the lengthy SQ-FEA driven along finite element method applied on the structure as a whole (SQ-STRU), they failed by losing the full accuracy. In addition, as already stated in Chapter 1, they treated separately the memory and the time. Hereinafter, it is proposed an SQ-FEA coupled with optimized substructuring technique (SQ-SUBS) that encompasses time and memory and provides a sizing method of the optimal substructure.

4.1 Substructuring Technique Theory

It is well known that dealing with large matrices requires much of the computer memory and operational time. Substructuring aspires to reduce the size of the involved matrices by dividing the entire structure into smaller substructures. Przemieniecki (1963) presented a matrix structural analysis of substructures and extensively described it in his book (Przemieniecki, 1968, pp 231-263). Later, He, Zhou and Hou (2008), and Leung (1979) used and recommended this technique to simplify the analysis of mega-structures.

Any given structure can be divided into n substructures separated by the boundaries constituting the set of nodes named boundary nodes. The remaining

nodes of each substructure are called interior nodes. So, for the r^{th} substructure, the well known equation

$$\mathbf{K}^{(r)}\mathbf{U}^{(r)} = \mathbf{P}^{(r)} \tag{4.1}$$

can be written as

$$\begin{bmatrix} \mathbf{K}_{bb}^{(r)} & \mathbf{K}_{bi}^{(r)} \\ \mathbf{K}_{ib}^{(r)} & \mathbf{K}_{ii}^{(r)} \end{bmatrix} \begin{Bmatrix} \mathbf{U}_{b}^{(r)} \\ \mathbf{U}_{i}^{(r)} \end{Bmatrix} = \begin{Bmatrix} \mathbf{P}_{b}^{(r)} \\ \mathbf{P}_{i}^{(r)} \end{Bmatrix}. \tag{4.2}$$

Here, **K**, **U** and **P** stand for stiffness, displacement and load while the subscripts b and i stand for boundary and interior, respectively. The boundary matrix of one substructure is obtained from

$$\mathbf{K}_{b}^{(r)} = \mathbf{K}_{bb}^{(r)} - \mathbf{K}_{bi}^{(r)}(\mathbf{K}_{ii}^{(r)})^{-1}\mathbf{K}_{ib}^{(r)}. \tag{4.3}$$

All these matrices are combined into a large one forming the stiffness boundary matrix $\mathbf{K}_b$ for the entire subdivided structure. After relaxation, the resultant boundary force matrix is

$$\mathbf{S}_b = \mathbf{P}_b - \sum_{r=1}^{n} \mathbf{K}_{bi}^{(r)}(\mathbf{K}_{ii}^{(r)})^{-1}\mathbf{P}_{i}^{(r)} \tag{4.4}$$

where $\mathbf{P}_b$ is the boundary force matrix corresponding to $\mathbf{K}_b$. The boundary displacements are determined from

$$\mathbf{U}_b = (\mathbf{K}_b)^{-1}\mathbf{S}_b. \tag{4.5}$$

Now, to calculate the interior displacements the boundary displacement matrix is divided into *n* substructure-boundary-displacement matrices, as

$$\mathbf{U}_{i}^{(r)} = (\mathbf{K}_{ii}^{(r)})^{-1}\mathbf{P}_{i}^{(r)} - (\mathbf{K}_{ii}^{(r)})^{-1}\mathbf{K}_{ib}^{(r)}\mathbf{U}_{b}^{(r)}. \tag{4.6}$$

Having obtained all node displacements, the rest of the analysis can follow within each substructure as the conventional displacement method. It can readily be observed that the sizes of matrices involved in this calculation are less than the sizes of the corresponding matrices involved in the entire-structure analysis (SQ-STRU).

Especially, the entire structure stiffness matrix is reduced provided that the interior nodes exist.

However, in the majority of cases there is no interior node in a floor. Since the efficiency of the substructuring technique is dependent on these interior nodes, it is necessary to take many floors as one substructure at a given stage of analysis. One should note that the lumped stories are not considered as constructed at the same time but regrouped only for the displacement determination. At this instant, only the penultimate floor weight is accounted as dead load self supported since the last floor is still shored up by formworks. Also, if the typical substructure consists of very few stories, the boundary matrix $\mathbf{K}_b$'s size will not so much differ from the whole stiffness matrix. On the other hand, if the substructure is too large, interior-to-interior submatrices $\mathbf{K}_{ii}$, which are mainly subjected to inversion, will also be too large. These two extreme cases will make the substructuring less efficient. The next section proposes a method which optimizes the substructuring. In other words, it will answer the question 'how to size the substructure to minimize the computation resources, say, time and memory'.

4.2 Combined Sequential Analysis and Substructuring Technique

Consider a 3D-frame building under its dead load and construction load as represented in Figure 4.1 given below. At any arbitrary construction stage, only the penultimate floor's weight is accounted for the analysis of the already-constructed part of the building which is analyzed by using substructuring technique. Therefore, Eq. (4.2) can be rewritten as

$$\begin{bmatrix} \mathbf{K}_{dd}^{(r)} & \mathbf{K}_{di}^{(r)} & \mathbf{K}_{du}^{(r)} \\ \mathbf{K}_{id}^{(r)} & \mathbf{K}_{ii}^{(r)} & \mathbf{K}_{iu}^{(r)} \\ \mathbf{K}_{ud}^{(r)} & \mathbf{K}_{ui}^{(r)} & \mathbf{K}_{uu}^{(r)} \end{bmatrix} \begin{Bmatrix} \mathbf{U}_{d}^{(r)} \\ \mathbf{U}_{i}^{(r)} \\ \mathbf{U}_{u}^{(r)} \end{Bmatrix} = \begin{Bmatrix} \mathbf{0} \\ \mathbf{P}_{i}^{(r)} \\ \mathbf{0} \end{Bmatrix}; \tag{4.7}$$

where the subscripts u and d stand for up and down boundaries, respectively. Note that for the first and all the intermediate substructures, $\mathbf{P}_i^{(r)} = \mathbf{0}$.

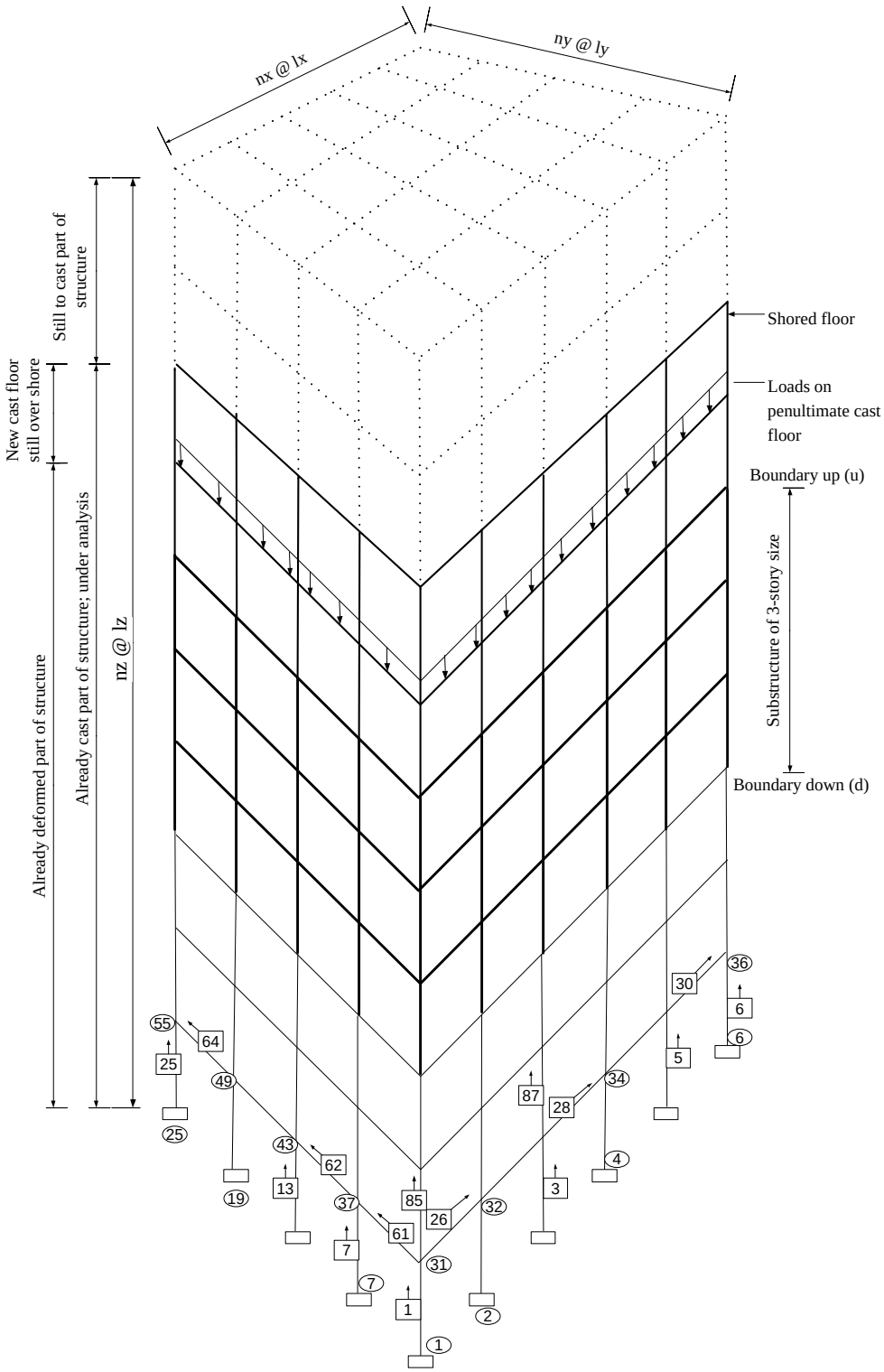

Figure 4.1. Representation of 3D-model building.

In this model, $\mathbf{K}_{st}^{(r)}$ $(s,t = d,u)$ is an $m \times m$ square matrix; the size $m = 6R$ where R is the number of columns at one floor level. For the actual case of a regular rectangular building footprint, $R = (nx + 1)(ny + 1)$, where nx and ny are the number of bays in X and Y directions, respectively. The rest of $\mathbf{K}_{st}^{(r)}$, where at least one of s or t is i, are either a $m' \times m$ / $m \times m'$ rectangular or a $m' \times m'$ square matrix. The maximum size is $m' = m(p-1) = 6(p-1)R$ with p denoting the number of stories constituting the substructure. Thus the size of each submatrix depends on R, the number of columns at any given floor level.

Remembering that in such a computation process the operation complexity depends on the size of the matrix, it is noticeable that the optimal size of substructure, p, will also depend on R. Considering only gravity loads during the construction, and a schedule in which each floor is stricken before the construction of the next one, two procedures have been developed in the computer algebra system Wolfram Mathematica version 7.0 running with a laptop working under Windows 7 Home basic, with a CPU Intel Core i5-480M, 2.66 GHz and a 4 GB RAM.

Procedure A considers SQ-FEA of buildings without substructuring (SQ-STRU) while procedure B considers substructuring (SQ-SUBS). Each of these procedures takes the stiffness matrix of each element in its current shape, as input. Then, after having constituted the convenient load matrix, it assembles all these stiffness matrices in the relevant form and yields the displacements.

With the values $nx = 5$ and $ny = 4$, and taking $p = 3$ and $p = 5$, Figure 4.2 has been plotted mapping various heights of the structure with the ratio of the time from procedure B over that from procedure A (Figure 2a), and the ratio of the memory from procedure B over that from procedure A (Figure 2b).

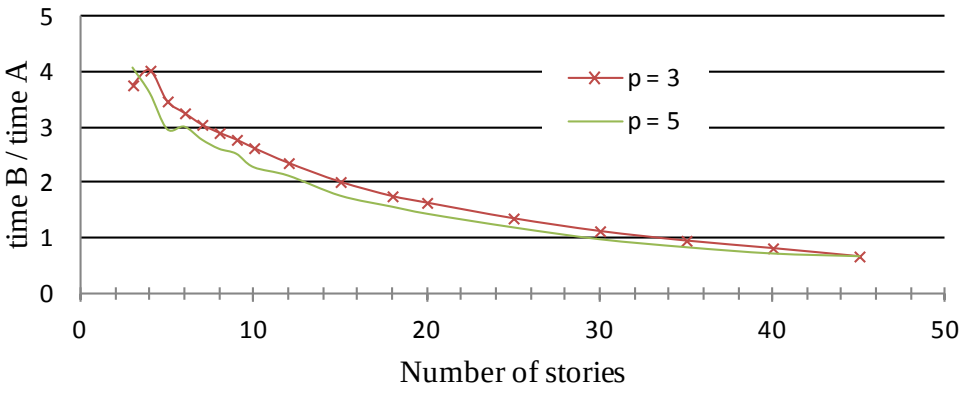

(a)

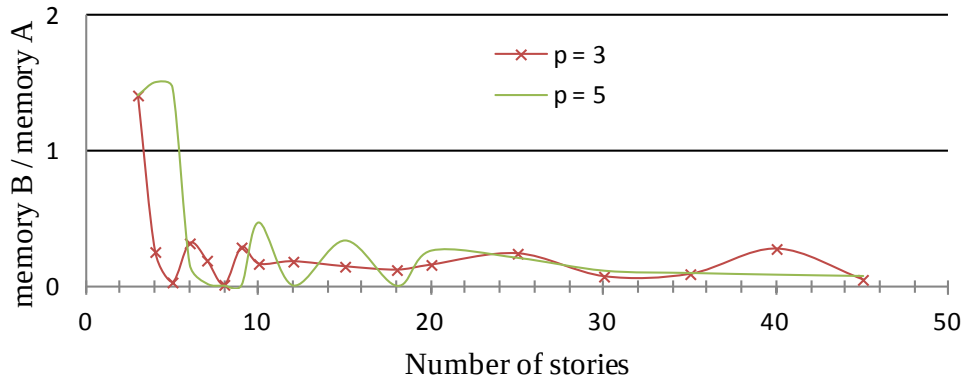

(b)

Figure 4.2. Comparison of computation resources. (a) Time. (b) Memory.

The results show that as the building's height becomes large, procedure B is more efficient than of procedure A as expected. Also, regarding the time, the packaging $p = 5$ is more advantageous. In addition, because the memory keeps fluctuating, there is no noticeable demarcation between the two packaging results and they are both unfavorable for low-rise buildings.

One important thing is that even if the computation requires much time, it is imperative to reduce the required memory as otherwise the computation would be impossible for the latter case while one waits continuously for the former. Hence, it is essential to make sure that the memory is always beneficial rather than systematically reduce the time.

For several structures, experiments have been conducted in order to determine the optimal substructure size. The graph shown in Figure 4.3 exhibits a stepped scatter whose steps respectively correspond to a particular range **R** of building footprint size. Although for a given range, all the graphical points have the same size, few experimental cases are widespread around the majority ones whose depicting points are massively superimposed and then draw three main pairs of lines. In others words, for each range, the greater part of the points, organized along a back bone around which few others points, actually represents many points upon the others. This plot has been therefore divided into 3 subplots matching the relevant range. Table 4.1 shows the equation of the regression line along with the p-value from the chi-squared test. Experiments have been carried out up to $\mathbf{R} = 180$ which can include almost all possible buildings; hence the last interval may be extended for special cases.

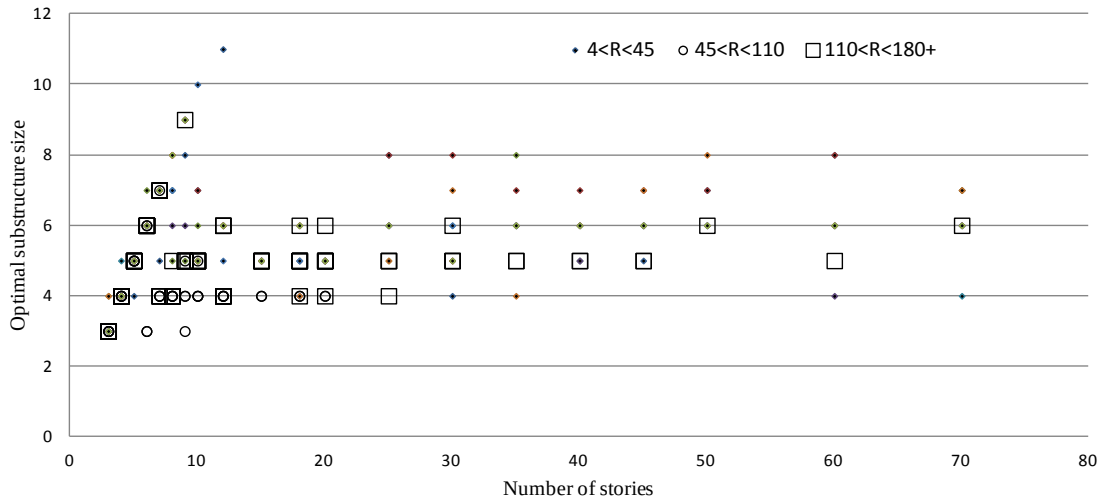

Figure 4.3. Experiment results in a stepped scatter shape.

The results show that for an arbitrary range of building footprint size, the optimal substructure size with respect to the time is equal to the number of stories of the whole structure under SQ-FEA when this story number does not exceed a certain critical value. This optimal substructure size seems to be a constant value as the

number of stories increases. For the case under study that corresponds to range 1, this observation is illustrated in Figure 4.4a. This reflects the fact that SQ-STRU is more efficient than SQ-SUBS for low-rise buildings, and for high-rise structures the latter is favorable. But as it was previously discussed, it is less appropriate to take the whole structure as substructure regarding the memory, which is capital to minimize. So, it is found more convenient to extend the second line backward to the point $(p+1, p)$ and then observe the minimum possible value $p = 2$ to handle all-number-of-story buildings as done in Figure 4.4b. Table 4.2 recapitulates the optimal substructure size for each range and for each interval of building height.

Table 4.1. Partitioning and regression equation line

Range	$\boldsymbol{a} \leq \mathbf{R} \leq \boldsymbol{b}$		Optimal substructure size, $\boldsymbol{p}$	Probability (p-value) from Chi-squared test
	a	b		
1	4	45	$\begin{cases} y = x, & x \leq 9 \\ y = 6, & x > 10 \end{cases}$	1.00 1.00
2	45	110	$\begin{cases} y = x, & x \leq 7 \\ y = 5, & x > 8 \end{cases}$	1.00 1.00
3	110	180+	$\begin{cases} y = x, & x \leq 6 \\ y = 4, & x > 7 \end{cases}$	0.96 1.00

Table 4.2. Optimal substructure size

Range	$\boldsymbol{a} \leq \boldsymbol{R} \leq \boldsymbol{b}$		Critical constant	Optimal substructure size	
	a	b	$\boldsymbol{p_0}$	$nz \leq p_0$	$nz > p_0$
1	4	45	6	2	6
2	45	110	5	2	5
3	110	180+	4	2	4

Figure 4.5 exhibits what would the results have been for the current study case if the model had not been corrected. The uncorrected model is favorable for the time but is prejudicial for the memory. Figure 4.6 presents how the corrected model behaves. Even though, in the earlier stage, it is not advantageous with respect to time, the memory is kept favorable throughout the whole process.

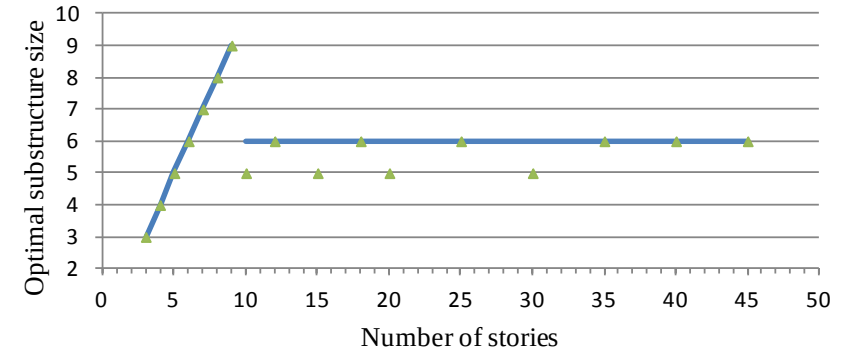

(a)

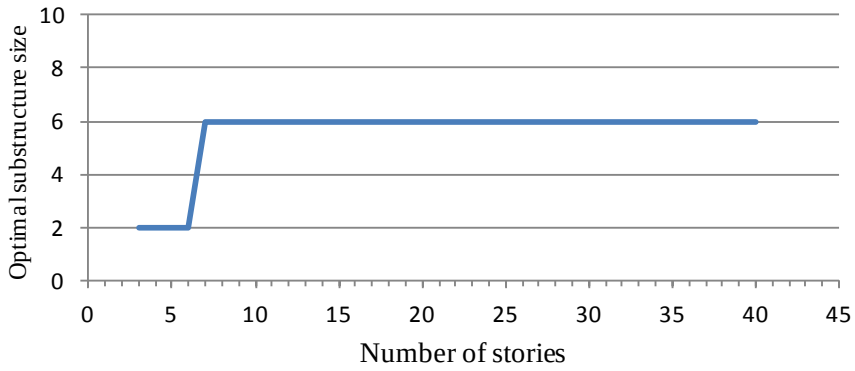

(b)

Figure 4.4. Optimization procedure results for the study case. (a) Uncorrected model. (b) Corrected model.

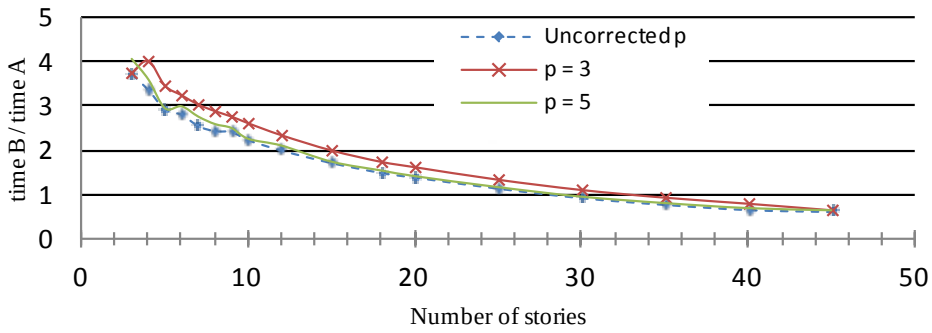

(a)

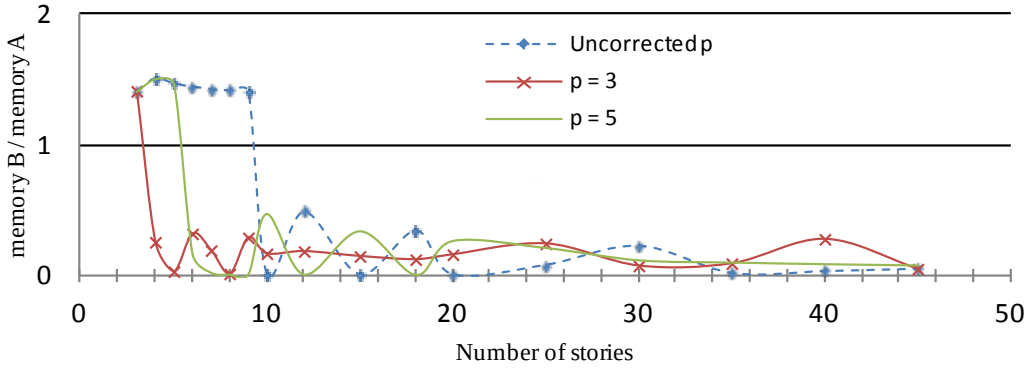

(b)

Figure 4.5. Comparison of computation resources - uncorrected optimization procedure. (a) Time. (b) Memory.

This model can be combined which other types of loads or effects such as aging, creep, shrinkage, construction loads and temperature action. The main operation steps used to implement the proposed sequential analysis coupled with optimized substructure technique are recapitulated in the flow chart given in Figure 4.8.

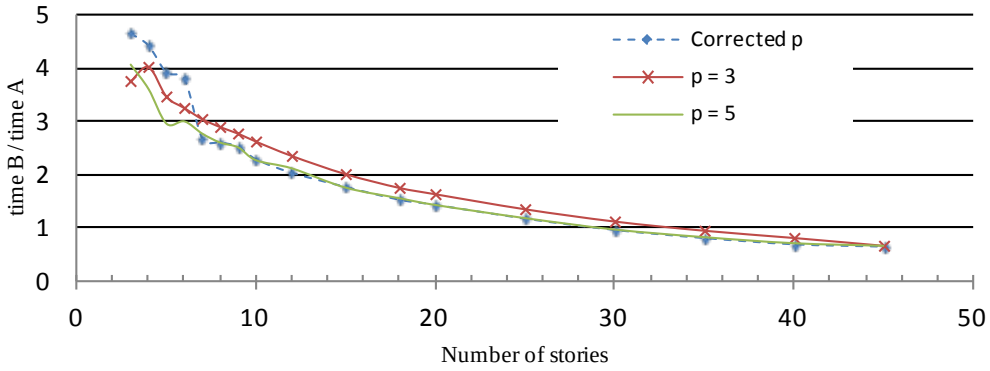

(a)

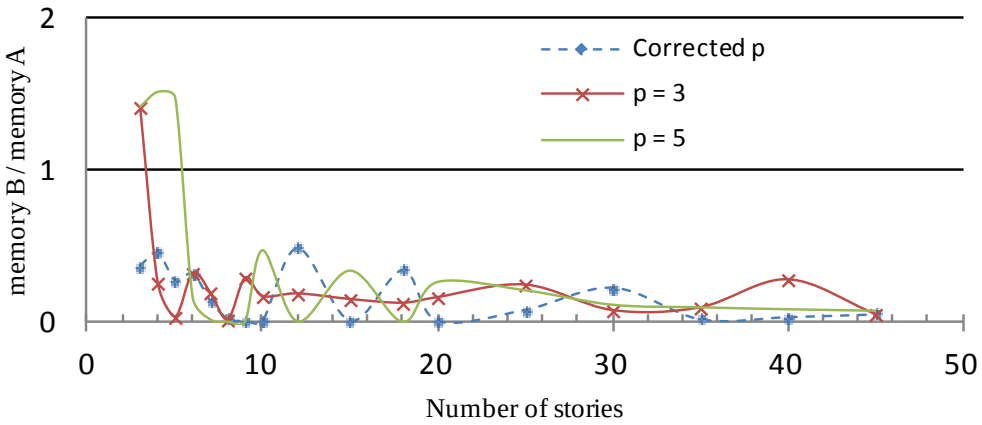

(b)

Figure 4.6. Comparison of computation resources - corrected optimization procedure. (a) Time. (b) Memory.

4.3 Numerical Cases

Table 4.3 below deals with three cases on which the proposed model is operated and the results are explained through the histogram shown in Figure 4.7. This figure lays out the percentage of computation resources out of those of SQ-STRU.

These charts show that for low rise buildings (case 1) the proposed model and the two other SQ-SUBS may require a longer time, more than 2 times that of SQ-STRU. The proposed model presents almost the same duration than the faster of the other SQ-SUBS but with most favorable memory use. Case 2 is the critical case where SQ-SUBS becomes more advantageous than SQ-STRU; needed amounts of time are very close but required quantities of memory use are almost 20% of that of SQ-STRU. The present method and the 5-by-5 procedure coincide due to the fact that the optimal packaging here is 5. Case 3 reflects a relatively larger structure where the proposed model is more competent and starts to widen the gap with SQ-STRU.

Table 4.3. Geometric characteristics of study cases

	Case 1	**Case 2**	**Case 3**
nx	4	10	4
***lx* (in meters)**	3.10	4.50	4.00
ny	6	5	6
***ly* (in meters)**	4.00	3.70	4.20
nz	10	25	40
***lz* (in meters)**	3.50	3.75	3.00
lx, ly and *lz* are the bay widths in X, Y, and Z direction, respectively.			

As promised, the question ‘how to size the substructure to minimize the computation resources, say, time and memory’ have found above an easy-to-apply answer. the SQ-SUBS procedure developed here keeps the full accuracy. But, even though it minimizes the memory while reducing the time with respect to those of SQ-STRU, it does not smooth the differences between SM-FEA and SQ-FEA. It could have been worthwhile to draw a bridge over these two last procedures with the intention to avoid the lengthy repeated analyses required by SQ-FEA while also keeping a good accuracy.

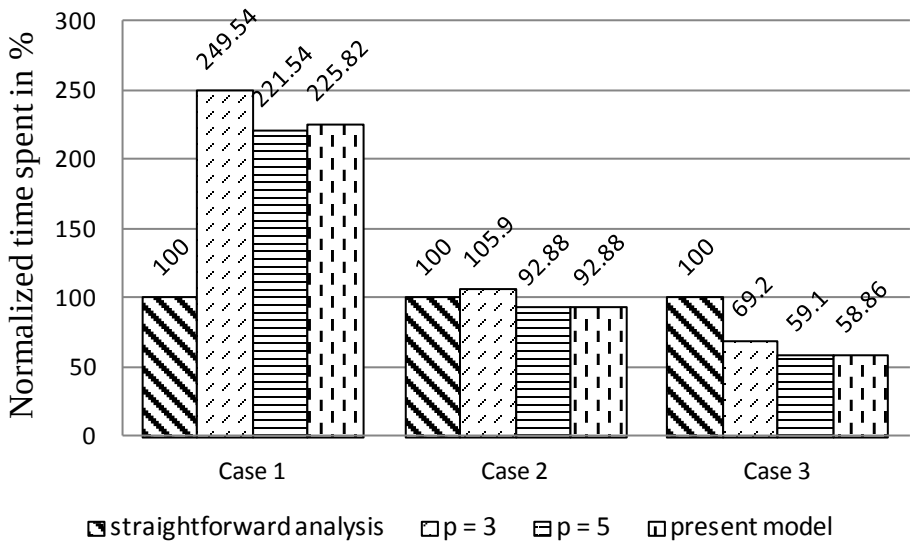

(a)

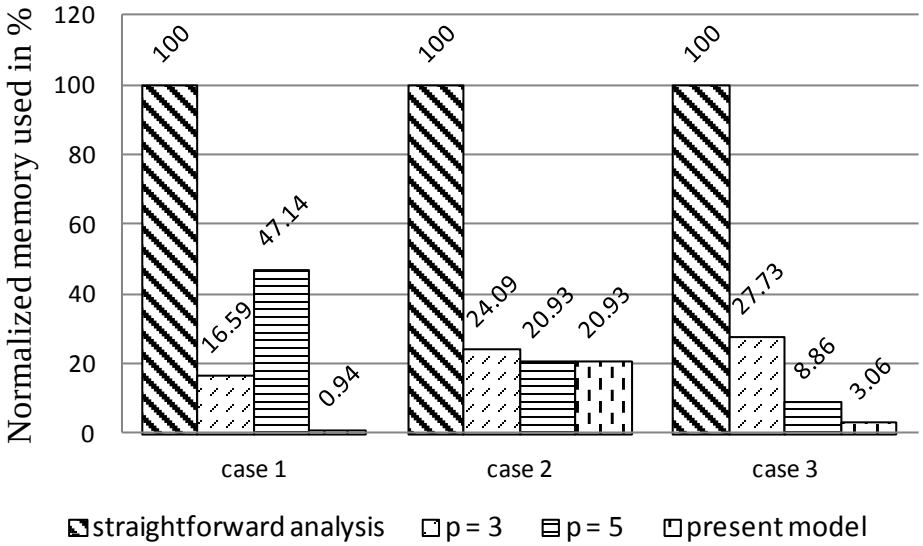

(b)

Figure 4. 7. Comparison of normalized computation resources - three numerical cases. (a) Time. (b) Memory.

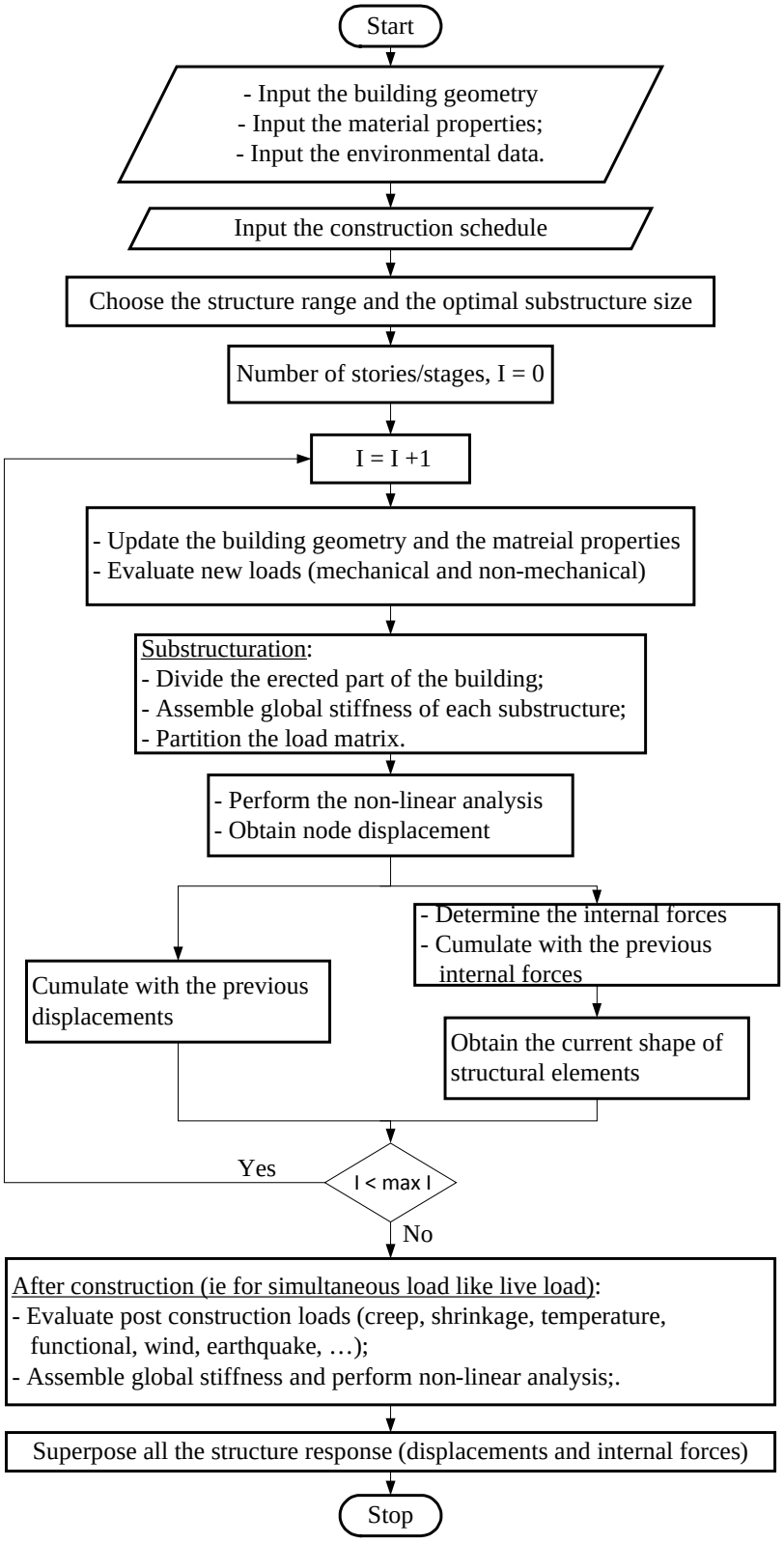

Figure 4.8. Main operation steps of the proposed model.

Chapter 5

NEURAL NETWORK: MINIMIZATION OF DIFFERENTIAL COLUMN SHORTENING AND RESULT PREDICTION

Obviously, the SQ-FEA process as presented in the previous chapters, introduced itself as being much complicated that the conventional analysis which is performed at one go. But it appears to be more accurate and the computational effort is justified for detailed phase analysis of a project management. However, for the initial design phase during which the accuracy is a luxury, structural engineers need to get structural response easily and quickly with a reasonable approximation. The main principle is to capture the relationship between simultaneous analysis results and those of sequential.

Within the framework of this chapter, it has been considered an ANN that aims to guess directly the erroneous forces between SM-FEA and SQ-FEA. So, just performing the simultaneous analysis allows the prediction with an acceptable tolerance of sequential analysis results, differential settlement and forces at the end a particular beam. Equilibrium equations at different nodes are sufficient to determine those for columns. In this study, axial forces along beam as well as shear forces for columns are not investigated since lateral forces applied on building are not considered.

5.1 Neural Network Theory

Human brains are able to complete so sophisticated tasks. To achieve all these, it is made of about one hundred of billions of neurons (http://en.wikipedia.org/wiki/Human_brain), nerve cells connected together through a large network. With the intention to mimic such a system, scientists developed an artificial neural network composed of processing units. The final result can mainly perform two specific tasks: pattern recognition and function approximation (Belic, 2012, pp 3-22). This last task is evidently for our concern.

ANN presents several units to the external world arranged in two layers: one for data input, the other for data output. The input nodes do not process. Sandwiched between the two external world related layers, there are hidden layers whose connections to other hidden layers or input/output units are strengthened or weakened by weights. The actual output out of a given processing unit is the image of the sum of weighted inputs minus the unit threshold through the activation function. Herein, output units received zero-value thresholds. Several functions may act as activation function but they need to be continuous, differentiable, monotonically non-decreasing and easy to derivate (Fausett, 1994). A typical function, complying with these requirements, is the bipolar sigmoid function $tanh(\cdot)$ which will be used for the current problems.

The weights as well as thresholds have to be set along an operation called training or learning. There are many types of ANN learning algorithm. Walcsak and Cerpa (1999) claimed that feedforward back propagation algorithm is superior to the others because of its robustness and its easy accessibility. This algorithm consists of adjust progressively the weights and thresholds in order to minimize the system energy based on gradient descent method.

After having presented an arbitrary pattern, the energy may be estimated from:

$$E_p = \frac{1}{2}\sum_{k=1}^{m}(t_k - y_k)^2, \quad (5.1)$$

where m is the number of output units, t is the target output value and y is the actual output. The minimization of this energy with respect to the network parameters, say the connection weights and unit thresholds, leads to the updating factors as described by Rumelhart et al (1986). Plus, it is involved a momentum term used to smooth out the learning parameter changes. At this step, a given parameter is obtained from

$$v_m(\tau + 1) = v_m(\tau) - \eta \frac{\partial E_p}{\partial v_m} + \alpha \Delta v_m(\tau), \quad (5\ 2)$$

in which v_m is the parameter under optimization, τ is the counter of the learning process, η is the gain fraction, α is the momentum term, and $\Delta v_m(\tau) = v_m(\tau) - v_m(\tau - 1)$.

As a supervised paradigm, all the input/output patterns of the training set should be presented to the network during the learning phase. One epoch designates a complete passage throughout the whole training set. The number of epochs may be used to characterize the learning process. It is necessary to precondition the patterns to have good performance. The input variables are scaled between [-1, 1] so that their respective mean values should be close to zero or else small compared to their respective standard deviation (Haykin, 2005) and the output are preprocessed to be within the range of the activation function avoiding saturation (Haykin, 2005; Belic, 2012).

5.2 Minimization of Differential Column Shortening

Choi and Kim (1985) and Choi et al (1992) remarked that the different tributary areas which exterior and interior column support, generate different loads upon these columns, approximately the double for internal columns. Since external columns are also robustly designed to withstand lateral forces, their shortening is moderate

compared to those of internal ones. This causes differential column shortenings in buildings. According to Fintel, Ghosh, and Iyengar (1986), the immediate consequence results in damages on non structural elements such as partitions especially light ones, architecture finishes and built-in furnishings, mechanical equipments and cladding. Also, the functionality and the visual aspect may be concerned. Wherefore, it is important to reduce this differential settlement.

5.2.1 Overview

Many factors characterize a particular project. These factors determine the structural response amongst which, displacements. Impacting on these displacements necessarily passes through the judicious adjustment of the relevant factors: environment, structure geometry and materials, and construction process. Environmental factors concern mainly temperature and relative humidity which are difficult to influence on. The general geometry of the edifice and members' sizes are dictated by the architectural and structural design. Generally, the material specifications to be used, say cement type and concrete grade, are specified in the tender documents or guided by the availability in the project location. The construction process, especially the interphase period between two typical stages, has a great impact on the total duration of the project, and, thus, on the total cost. Haroglu et al (2009) claimed that it is the structural engineer who is the most influential in selecting the correct structural frame for a project's feasibility and success. Therefore, he should propose a typical duration characterizing the construction timing. In short, it is convenient to minimize the differential shortening by choosing a suitable elementary duration since the other factors are awkward to be imposed or modified.

By considering a very short period of time between two stages, the concrete is still weak when receiving loads, and, thus, is much subjected to instantaneous deformations. On the other hand, if one waits too much between two stages, he allows temperature to change a lot and induces more stresses across the members. Here, the daily variations on temperature are considered negligible since they are generally small and they do not have enough time to penetrate across member's sections. Also, a high amount of temperature change may cause more shrinkage effects. By increasing internal forces and keeping for a long period of time construction loads applied on story below, one will result in more instantaneous deformations and more creep effects over the lengthy phase. Obviously, there is an optimal interphase between these two extreme cases that yields to a minimum maximorum differential shortening; since it is suitable to minimize the differential shortening at the member location it is more critical.

5.2.2 Illustrative Example

The same L-shaped 15-story office building of Section 3.3.1 is held here. But now, the elasticity modulus at 28 days has been obtained from Section 2.5.3 of the present thesis and became $E_C(28) = 27\,050\ MPa$.

Different analyses have been made with the commercial structural analysis software package SAP2000 version 15.1.0. The interphase has been varied from 1 to 28 days. That is, for a given interphase, the analysis has been conducted and the maximum differential column shortening has been noted as result. The graph in Figure 5.1 represents the evolution of the maximum differential shortening versus the interphase. It readily appears that the minimum occurs for the critical interphase of 10 days.

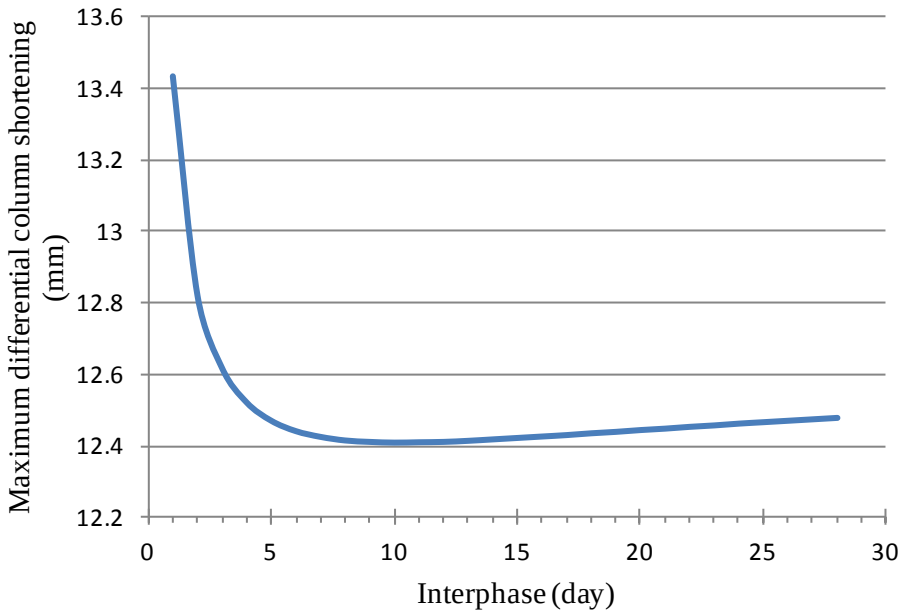

Figure 5.1. Evolution of maximum differential shortening versus interphase.

5.3 Implementation of Neural Network

One hundred of different buildings have been analyzed using SAP2000 version 15.1.0. The various determinant parameters have been chosen within practical ranges. 389 patterns are obtained from these analyses. 273 of them are used as training set, 58 as validation set and 58 as testing set. To implement back propagation feedforward ANN, routines have been written using the computer algebra system Wolfram Mathematica version 7.0.

5.3.1 Input Data

At a first approach and getting inspiration from the partial conclusion of Chapter 2 concerning non-lateral loads, parameters from environment, material properties, building geometry and construction process have been chosen to model the problem, as presented in Table 5.1. The results from sensitivity analysis are also reported. Also, it is noteworthy to precise that relative humidity and temperature are not related since one can find some geographical areas with the same temperature average but different humidity, and vice versa

(http://dailyapple.blogspot.com/2008/07/apple-328-its-humidity.html; http://en.wikipedia.org/wiki/File:Annual_Average_Temperature_Map.jpg).

Table 5.1. Input data for modeling

#		Parameters	Range	Sensitivity results
1	Environment	Relative humidity (%)	[0, 100]	sensitive
2		Temperature (°C)	[-110, +110]	sensitive
3	Material properties	Cement type	{0.20, 0.25, 0.38}	sensitive
4		Concrete grade (MPa)	[15, 50]	sensitive
5	Building geometry	Building height (number of stories)	[2, 20]	sensitive
6		Width of beam (mm)	[100, 350]	sensitive
7		Depth of beam (mm)	[150, 700]	sensitive
8		Length of beam (mm)	[500, 15000]	sensitive
9		Position of beam	{intermediate, middle, exterior}	Sensitive
10		Story of beam	[1, 20]	Sensitive
11	Construction process	Interphase (days)	[1, 28]	Sensitive
12		Date of shrinkage start		Non sensitive

The sensitivity analysis reveals that the age of concrete at the beginning of the shrinkage is not sensitive, so this parameter has not been considered in this study. The cement type here is denoted by its characteristic coefficient as reported in Table 2.3. Ali and Moon (2007) argued that for cost-efficiency the maximum number of stories of R/C frame building is 20 stories, and it is not relevant in this study to deal with single-story buildings. http://www.mherrera.org/temp.htm recapitulates the extreme temperatures around the world. It presented the extreme temperature change of $\pm$104.9℃ as occurring in Verkhojansk, Russia. But, as Anderson et al concluded in 1997, this range has been little enlarged with the intention to allow the network to handle the edge of data space, and to foresee special cases (potentially due to uncertainties of measures or global warming). However, the interphase has been restricted under 28 days due to the symbolism carried by this age of concrete.

Since, it is necessary to normalize, all have been scaled between [-1, 1]. Two variables experienced a specific preprocessing treatment. By convention specific to this study, the position of the beam has been coded -1 for intermediate, 0 for middle and +1 for exterior. Apart the cement type which has been directly scaled such that 0.2 corresponds to -1, 0.25 to -4/9, and 0.38 to +1, the remaining parameter ranges have been sized into [-1, 1] using the log/antilog strategy because of the wide range (several decades) of their natural collections (Leondes, 1998). With such wide ranges taken into [-1, 1], some variables will be confined within subparts and will not differ enough to be efficiently handled by the network; thus, they need to be redistributed along the entire bipolar interval. As the decimal logarithm tends to separate small but close numbers, and, also, tends to bunch greater ones, Equation (5.4) has been developed to propose in this study a bijective function which keeps both variables' sign and order as well as it achieves the required equal distribution. Therefore, preconditioned values are obtained from:

$$x' = \frac{2(lg\, x - lg\, x_{min})}{lg\, x_{max} - lg\, x_{min}} - 1, \tag{5.3}$$

where x is the natural value, and x_{max} and x_{min} are the maximum and minimum natural values of the corresponding input, respectively. $lg(\cdot)$, which involves the decimal logarithm $log_{10}(\cdot)$, is defined as:

$$\lg(z) = \begin{cases} -\log_{10}(|z-1|), & z < 0 \\ \log_{10}(z+1), & z \geq 0 \end{cases}. \tag{5.4}$$

5.3.2 Output Data

Based on the targeted objectives, Table 5.2 displays the possible final output. The output data are scaled into $[-1 + S_m, +1 - S_m]$. S_m is the saturation margin at each bound of the interval and is taken as $S_m = 0.01$. Therefore, the preprocessed values are given as:

$$y' = \frac{2(1-S_m)(lg\, y - lg\, y_{min})}{lg\, y_{max} - lg\, y_{min}} - (1 - S_m), \tag{5.5}$$

and the postprocessed or natural values:

$$y = gl(\frac{(lg\, y_{max} - lg\, y_{min})(y' + 1 - S_m)}{2(1-S_m)} + lg\, y_{min}); \tag{5.6}$$

$$gl(t) = \begin{cases} 1 - 10^{-t}, & t < 0 \\ -1 + 10^{t}, & t \geq 0 \end{cases}. \tag{5.7}$$

In Equations (5.3), (5.5) and (5.6), $lg(\cdot)$ is the function as defined in Equation (5.4), $gl(\cdot)$ is the inverse function of $lg(\cdot)$, and y_{max} and y_{min} are the maximum and minimum natural values of the corresponding output, respectively.

Table 5.2. Output data for modeling

#	Parameters	Range
a	Optimal interphase (day)	[4, 28]
b	Erroneous diff. col. shortening (mm)	[-6, 3]
c	Erroneous moment at node 1 (kNm)	[-100, 165]
d	Erroneous moment at node 2 (kNm)	[-135, 75]
e	Erroneous shear force at node 1 (kN)	[-60, 40]
f	Erroneous shear force at node 2 (kN)	[-30, 195]

5.3.3 The Training Process

For each (sub-) problem, the numbers of exterior nodes are fixed by the problem itself. But there is neither any deterministic method to set the number of hidden layers, nor any one for the number of nodes within each hidden layer. Although theoretically a unique hidden layer with sufficient nodes can be efficient as claimed by Walczak and Cerpa (1999), Belic (2012), and Fausett (1994), it may be convenient to have more hidden layers in order to handle more complexities in the hyperspace (Walczak and Cerpa, 1999; Fausett, 1994).

However, there are some heuristic principles, which have been reported by authors, that guide the setting up of the interior ANN size: using 75% of the quantity of input nodes (Walczak and Cerpa, 1999), or using 50% of the quantity of input and output nodes (Walczak and Cerpa, 1999), or using $2n + 1$ hidden nodes where n is the number of nodes in the input layer (Walczak and Cerpa, 1999), or else using as the number of weights to be trained $P \times e$, where P is the number of training patterns, and e, the accuracy of classification expected (Fausett, 1994).

Anyway, different trials are necessary to obtain the most efficient architecture. Some authors suggest starting with a small number of nodes, and increase them in number till the network performs well. Others recommend, on contrary, to select a huge number, and prune the network as its performance get better. This last solution can be also reached by adopting the so-called weight elimination technique which aims to push to zero the connection weights related to useless nodes, so to prevent them for any participation. It consists of modification of the network energy from Equation (5.1) to $W = \sum_p E_p + 0.5\,\lambda \sum_m \frac{(\frac{v_m}{v^*})^2}{1+(\frac{v_m}{v^*})^2}$, thus Equation (5.2) becomes, for connection weights only (thresholds are not concerned):

$$v_m(\tau + 1) = v_m(\tau) - \eta \frac{\partial E_p}{\partial v_m} + \alpha\, \Delta v_m(\tau) - \eta \frac{\lambda}{v^*} \frac{\frac{v_m}{v^*}}{\left[1+(\frac{v_m}{v^*})^2\right]^2}, \quad (5.8)$$

with λ and v^* are constants.

Also, it is a tremendous task to choose the initial values of weights and thresholds to start the training process. But to avoid saturation, they should be small enough (Haykin, 2005). Fausset (1994) recommended setting them randomly between -0.5 and 0.5. Then, a simple modification as developed by Nguyen and Widrow in 1990 is accounted. If n and h are the numbers of input and hidden units, respectively, the scale factor $\beta = 0.7\sqrt[n]{h}$ and the column norm into the input-hidden weight matrix

$\|w_j\| = \sqrt{\sum_{i=1}^{n} w_{ij}^2}$, where w_{ij} is the weight from input unit i to hidden unit j. Then the reinitialized weights will be $w_{ij} \leftarrow w_{ij} \times \beta / \|w_j\|$ and the unchanging thresholds for hidden units remain randomly chosen between $-\beta$ and β. Weights to output units and thresholds are not subjected to this modification.

Finally, learning rate η and momentum α are as well, a result from many tentative trials although Anderson et al (1997) suggested to take $\eta = 1/n$ and $\alpha = 3/(2n)$ where n is the number of input nodes.

Once launched, the training has been stopped for one of these three reasons arranged in order of priority: (1) the validation energy starts to increase; (2) the training energy drops under an arbitrary tolerance, say 10^{-6}; (3) a given number of epochs, 10^8, is reached.

In line with the energy defined in Equation (5.1), the error at each output node, after the presentation of the last epoch that corresponds to the end of the training phase, is calculated from:

$$error = \frac{0.5}{P \times m} \sqrt{\sum_{j=1}^{P} \sum_{k=1}^{m} (t_k - y_k)^2}, \tag{5.9}$$

where m, t and y are defined as in Equation (5.1), and P is the number of patterns.

Instead of using a commercial software package, all these references and techniques have been considered to code a program from which two nets have been designed, each for different tasks: minimization of differential shortening and structural response prediction.

5.3.4 Minimization of Differential Shortening

For the differential shortening minimization, a network with a single architecture has been obviously held. As input data, parameters that describe the project in hand as a whole are used: items 1-5 from Table 5.1. The expected output is the optimal

interphase yielding to minimum maximorum of differential column shortening. Since this optimal interphase has been ceiled at 28 days, the ANN is tending to reduce a bit the actual output but still keeping a good accuracy. Table 5.3 below points out the results obtained. Using the highlighted net in this Table 5.3, Figure 5.3 has been drawn. The relative position of each point with respect of the 45° line shows how well the approximated prediction fits with the perfect expected value.

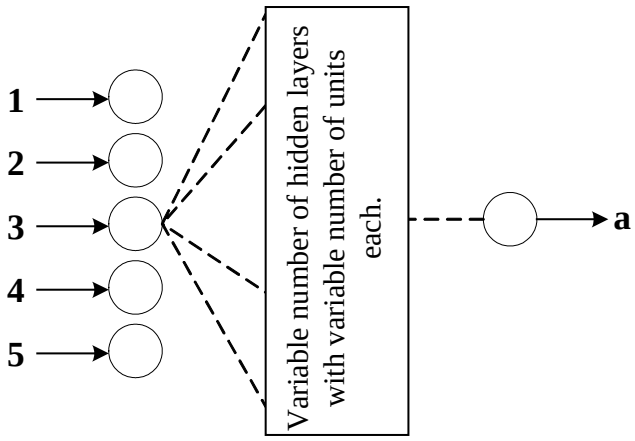

Figure 5.2. Typical configuration of ANN for minimization of differential shortening.

Table 5.3. Differential shortening Minimization ANN's training results

Configuration	Number of epochs	Training error	Validation error	Generalization error
5-15-1	28	0.00418	0.00912	0.01095
5-15-1-1-1	**1294**	**0.00279**	**0.00728**	**0.00636**
5-5-20-4-1	2137	0.00266	0.00744	0.00658
η = 0.100; α = 0.020; λ = 0.00 or 0.01; v^* = 3.00				

Numerical Case

The study case described in Section 5.2.2 is recalled here to serve as checking case of the ANN designed above. As depicted in Figure 5.1, the optimum interphase is 10 days. The prediction obtained is 9.95 days. Considering the aforementioned fact about the capping of interphase, this result is definitely acceptable.

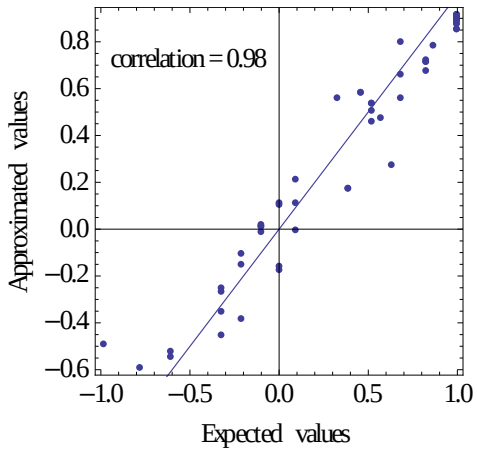

Figure 5.3. ANN 1: mapping expected values versus ANN results.

5.3.5 Structural Response Prediction

This neural network aims to predict all the needed data, b – f from Table 5.2, using input data 1 - 11 in Table 5.1. Here are reported the analysis results in Table 5.4. As in the first problem, Figure 5.5 has been produced from the network in bold face of Table 5.4. The correlation between the ANN prognostics and the FEM results is 0.89.

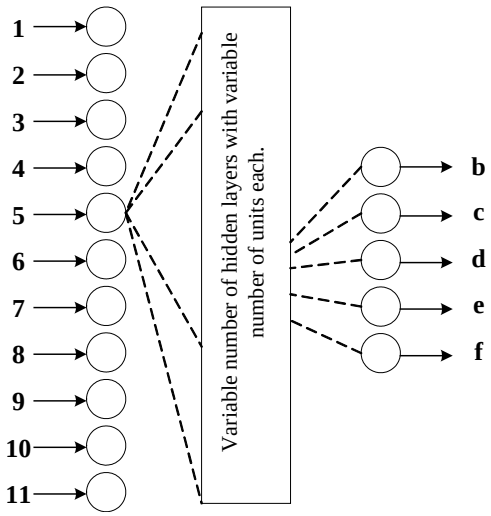

Figure 5.4. Typical configuration of structural response ANN.

Table 5.4. Structural response ANN's training results

Configuration	Number of epochs	Training error	Validation error	Generalization error
11-50-50-50-5	468	0.00171	0.00360	0.00431
11-20-20-20-5	915	0.00175	0.00338	0.00460
11-35-45-35-5	**1198**	**0.00138**	**0.00329**	**0.00431**
η = 0.100; α = 0.020; λ = 0.00; v^* = 3.00				

Table 5.5. Illustration and description of the numerical case #2

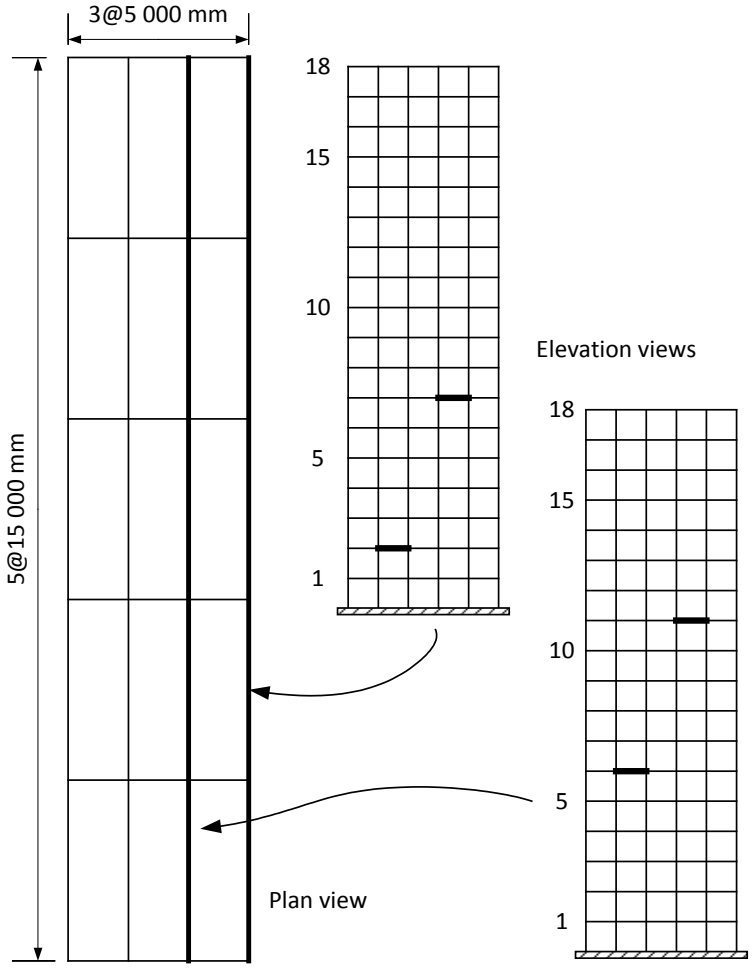

Relative Humidity = 59%	**Concrete grade** = 28 MPa	**Position**: intermediate
Temperature change = 23°C	**Building height** = 18 stories	**Holder story** = 2, 6, 7 or 11
Cement type = 0.38	**Beam** 250×650×15 000 mm^3	**Interphase** = 23 days

Numerical Case

A numerical case is taken to show the prediction performance of this neural network. Table 5.5 illustrates and describes the building in hand, Table 5.6 reports the different results obtained from various methods herein considered, and Table 5.7 states the errors observed in SQ-ANN compared to SQ-FEA. These errors, expressed in percent (%), vary from -2.34 to 2.63, values which are acceptable regarding the simplicity of this method.

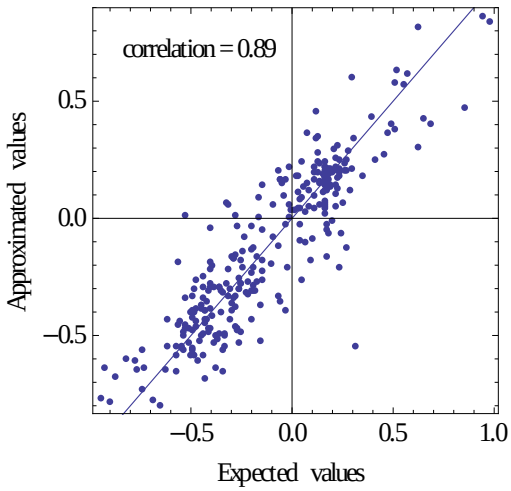

Figure 5.5. ANN 2: mapping expected values versus ANN results.

Table 5.6. Result report for numerical case #2

		Story 2		Story 6		Story 7		Story 11	
		Node 1	Node 2	Node 1	Node 2	Node 1	Node 2	Node 1	Node 2
Differential settlement (mm)	**SM-FEA**	2.729		7.162		8.067		10.906	
	SQ-FEA	3.688		9.205		10.118		11.987	
	SQ-ANN	3.898		8.963		9.794		12.147	
Moment (kNm)	**SM-FEA**	-394.85	-436.85	-418.96	-412.05	-422.42	-408.09	-433.36	-395.74
	SQ-FEA	-377.26	-412.81	-397.29	-393.19	-400.07	-390.65	-406.53	-386.67
	SQ-ANN	-383.78	-403.82	-399.27	-383.98	-399.21	-386.28	-397.89	-389.56
Shear force (kN)	**SM-FEA**	-133.38	138.98	-136.23	135.41	-136.66	134.87	-138.03	133.19
	SQ-FEA	-123.93	128.30	-126.56	126.01	-127.00	125.78	-128.28	125.76
	SQ-ANN	-126.08	131.94	-129.55	123.42	-129.46	123.85	-128.62	126.10

Table 5.7. Percentage errors in results for numerical case S2

	Story 2		Story 6		Story 7		Story 11	
	Node 1	Node 2	Node 1	Node 2	Node 1	Node 2	Node 1	Node 2
Differential settlement	5.69		-2.63		-3.20		1.33	
Moment	1.73	-2.18	0.50	-2.34	-0.21	-1.12	-2.13	0.75
Shear force	1.73	2.84	2.36	-2.06	1.94	-1.53	0.27	0.27

Chapter 6

CONCLUSION AND RECOMMENDATIONS

6.1 Summary

Throughout this thesis, many problematics have been considered around sequential analysis. The first one was the presentation of this theory and the highlighting of its significance. Here, a strategy on how to conduct this analysis has been proposed, considering the realistic situation under which actual R/C 3D frames building are subjected including various common loads. The individual contributions of these loads have been investigated on a study case, not each separately, but sequentially as they are applied in situ.

The second problem dealt with an accurate process aiming to reduce the computational resources required to perform sequential analysis, say memory and time. The substructuring technique as proposed as Przemieniecki (1968) has been reformulated and coupled to sequential analysis without any loss of accuracy.

Since sequential analysis is firmly related to differential column shortening phenomenon, the third goal aimed to reduce it by a carefully selection the interphase that leads to minimum maximorum differential column shortening. For this purpose, an artificial neural network has been designed; it takes as inputs general and easy-to-get project's parameters and brings out the said optimal interphase. Another artificial neural network has been put up with the intention to predict sequential analysis results from those of simultaneous one. It has been found out that these tools are useful at the preliminary design stage.

6.2 Conclusion

After peeling out various loads, findings are alarming. These following major lines can be stated.

- For beams located at lower floor, SQ-FEA's and SM-FEA's moments are not divergent, but they are for upper floor where a 62% difference can be observed.
- SQ-FEA results show that moments are actually more distributed along continuous beams than SM-FEA seems to demonstrate.
- The difference between the two analyses is more sensitive with irregularities in buildings.
- This difference is moderated when applying live load.
- Temperature actions happened to be of great importance for the lower stories where a change of 50% can be noticed in the second floor, and a different behavior may arise in the first one since the moment's sign may be inversed, from -65.36 kNm to +14.49 kNm for example. Although their effect can be neglected for the upper stories, the final moment curve is more influenced, even dictated, by the temperature curve when it is considered.
- From top to bottom, time dependent effect and construction loads induce greater change on moments computed when they are ignored. Altogether, they may equally share a change in moments of 65%.
- Earthquake action does not significantly vary from one analysis to another.

These points prove that, when statically analyzing a building, the nonlinearity caused by the sequential application of loads has to be accounted. Furthermore, all the various loads investigated here happened to play great role such that there will be a serious default if not.

Nevertheless, SQ-FEA required computational consuming process. To overcome this problem, an algorithm has been proposed to help engineers to easily implement this process in an optimal manner. From the statistical analysis of the experiments which coupled sequential analysis and substructuring technique, the result has been the conception of a simple process based on the choice of the optimal substructure size. With the study cases that have been considered, up to 42.14% of time amount and 99.06% of memory amount have been saved.

But this is still tedious when the full accuracy is not required. A soft computing tool, well known as artificial neural network, has been used here to cope this case. Instead of using a commercial software package, many references providing advanced principles have been considered to code a program. Without any analysis, but just by considering five general parameters to characterize a given project, the optimal interphase can be predicted with a very short time computation.

In addition, in order to avoid repeated analyses required by sequential analysis, whose procedure demands intricate modeling and long waiting time of analysis, its results can be deducted from those of simultaneous one by the means of another ANN. For one or the other, errors have been kept under 0.01 and correlation above 0.89. ANNs exempt engineers from full structure modeling for each change and/or analysis, but offer an acceptable accuracy in results by a second-duration computation.

6.3 Recommendation for Further Works

The sizing procedure developed here for substructuring considers only gravity loads occurring during the construction phase. It may be important to extend it to all the various loads. Also, it has been proposed based on regular rectangular 3D frames, further studies can investigate the case of vertically irregular ones.

The database which has been used for neural network training and validation, concerned only residential / office buildings with neither vertical irregularity nor circular part. Other networks can be set up considering these features.

In addition, training and validation sets have been chosen only amongst R/C buildings. Other constituting materials such as steel, prestressed concrete, or timber could be accounted to extend the range of these networks.

REFERENCES

Ali MM, & Moon KS. (2007). Structural developments in tall buildings: current trends and future prospects. *Architecture Science Review*. 50 (3), 205-23.

Anderson D, Hines EL, Arthur SJ, & Eiap EL. (1997). Application of artificial neural network to prediction of minor steel connections. *Structures & Computers*. 63(4), 685-92.

Association Française de la NORmalisation. Eurocode 1 : "Bases de Calculs et Actions sur les Structures" et Documents d'Application Nationale. AFNOR 2000. Tour Europe 92049 Paris La Défense Cedex.

Association Française de la NORmalisation. Eurocode 8 : Conception et dimensionnement des structures pour leur résistance aux séismes et documents d'application nationale. Partie 1. AFNOR 2000. Tour Europe 92049 Paris La Défense Cedex.

Azkune M, Puente I, & Insausti A. (2007). Effect of ambient temperature on the redistribution of loads during construction of multi-storey concrete structures. *Engineering Structures*. 29, 933-41.

Ballal TMA, & Sher WD. (2003). Artificial neural network for the selection of buildable structural systems. *Engineering, Construction and architectural management*. 10 (4): 263-71.

Belic I. (2012). Neural networks and static modeling. In: ElHefnawi M, Mysara M, editors. Recurrent neural networks and soft computing. Croatia: InTech. p. 3-22.

Choi CK, Chung HK, Lee DG, & Wilson EL. (1992). Simplified building analysis with sequential dead loads-CFM. *Journal of Structural Engineering ASCE*. 118(4), 944-54.

Choi CK, & Kim ED. (1985). Multistory frames under sequential gravity loads. *Journal of Structural Engineering ASCE*. 111(11), 2373-84.

Comite Euro-International du Beton. (1993). CEB-FIP Model Code 1990, Design Code. London: Thomas Telford Services Ltd.

Fausett L. (1994). Fundamentals of neural networks: architectures, algorithms and applications. New Jersey: Prentice-Hall.

Fintel M, Ghosh SK, & Iyengar H. (1986). Column shortening in tall structures – prediction and compensation. Portland cement association.

Fu XY, Wu B, Chen XC, Meng ML, Sun C, Jiang HB, Gao Y, & Li JW. (2008). Research on structural design of a super high-rise building in Qatar. *The IES Journal Part A: Civil & Structural Engineering.* 1(3), 186-97.

Gupta T, & Sharma RK. (2011). Structural analysis and design of building using neural network: a review. *International Journal of Engineering and Management Sciences*. 2(4), 216-20.

Haroglu H, Glass J, Thorpe T, & Goodchild C. (2009). Who is the key decision maker in the structural frame selection process? In: Limbachiya, Kew, editors. Excellence in concrete construction through innovation. England: Taylor & Francis Group. p. 119-26.

Haykin S. (2005). Neural network – A comprehensive foundation. 2nd ed. India: Pearson Education Inc.

He Y, Zhou X, & Hou P. (2010). Combined method of super element and substructure for analysis of ILTDBS reticulated mega-structure with single-layer latticed shell substructures. *Finite Elements in Analysis and Design*. 46, 563-70.

http://dailyapple.blogspot.com/2008/07/apple-328-its-humidity.html. Last accessed on August 10th, 2012.

http://en.wikipedia.org/wiki/File:Annual_Average_Temperature_Map.jpg. Last accessed on August 10th, 2012.

http://en.wikipedia.org/wiki/Human_brain. Last accessed on August 10th, 2012.

http://www.climatetemp.info/cyprus/famagusta.html. Last accessed on March 09th, 2012.

http://www.mherrera.org/temp.htm. Last accessed on August 10th, 2012.

Iliadis L, & Jayne C, editors. (2011). Engineering applications of neural networks. Part 1. London: Springer.

Kim HS, & Shin SH. (2011). Column shortening analysis with lumped construction sequences. *Procedia Engineering*. 14, 1791-98.

Kwak HG, & Kim JK. (2006). Time-dependent analysis of RC frame structures considering construction sequences. *Building and Environment*. 41, 1423-34.

Leondes CT. (1998). Optimization techniques. California: Academic Press.

Leung YT. (1979). An accurate method of dynamic substructuring with simplified computation. *International Journal for Numerical Methods in Engineering*. 14:1241-56.

Liu NX, Zhao X, Sun HH, Zheng YM, & Ding JM. (2011). Structural performance assessment and control of super tall buildings during construction. *Procedia Engineering*. 14, 2503-10.

Rumelhart DE, Hinton GE, & Williams RJ. (1986). Learning internal representations by error propagation. In: Parallel Distributed Processing Vol. 1: Foundations. The MIT Press, MA.

Solomos G, Pinto A, & Dimova S. (2008). A Review of the Seismic Hazard Zonation in National Building Codes in the Context of Euro code 8. Luxembourg: Office for Official Publications of the European Communities.

Ozay G, & Njomo W. (2012a). Minimization of differential column shortening and sequential analysis of RC 3D-frame using ANN. *Structural Engineering and Mechanics* (submitted for review).

Ozay G, & Njomo W. (2012b). Sequential analysis coupled with optimized substructure technique on 3D-frame construction process. *Engineering Structures*. (submitted for review).

Przemieniecki JS. (1963). Matrix structural analysis of substructures. *J. Am. Inst. Aeron. Astron*. 1,138-47.

Przemieniecki JS. (1968). Theory of matrix structural analysis. New York: McGraw-Hill Book Company.

Walczak S, & Cerpa N. (1999). Heuristic principles for the design of artificial neural networks. *Information and software technology*. 41, 107-17.